TECHNICAL UNIVERSITY OF GABROVO

Faculty of Electrical Egineering and Electronics

Dipl. Eng. Rumyana angelova Stoyanova

"DEVELOPMENT OF INNOVATIVE METHODS AND MECHANISMS FOR ENERGY PIEZOHARVESTERS"

AUTHOR's ABSTRACT

Of a dissertation for awarding an educational and scientific degree Ph. Doctor

Field of high education: 5. Technical Sciences

Professional direction: 5.2 Electrical Engineering, Electronics and Automation

Doctoral program: „Microelectronics"

Scientific supervisors

1). Associate Professor PhD Dipl. Eng. Velimira Dimitrova Todorova

2). Professor PhD Dipl. Eng. Anatoliy Trifonov Aleksandrov

Reviewers:

1). Professor PhD Dipl. Eng. Ivan Borisov Evstatiev
2). Associate Professor PhD Dipl. Eng. Nikola Draganov Draganov

Gabrovo 2024

The dissertation work has been discussed and directed for official defense at a meeting of the Extended Departmental Council of the Department of "Electronics at the faculty "Electrical Engineering and Electronics" of Technical University - Gabrovo, held on 15.10.2024.

The dissertation contains 160 pages. The scientific content is presented in an introduction, four (4) chapters and, a conclusion, includes 180 figures and 77 tables. 200 literary sources are cited. The numbering of figures, tables and formulas in the abstract is consistent with those in the dissertation

The research on the dissertation work was carried out in the Department of “Electronics” at the Faculty of "Electrical Engineering and Electronics" and “Mechanical Engineering and Instrument Engineering” at the Faculty of ”Mechanical engineering and instrument Engineering” of the Technical University – Gabrovo.

The official defense of the dissertation work will take place on 02/07/2025 from.....h., in room.....of the Technical University - Gabrovo.

Rumyana Angelova Stoyanova- author, 2024
Title: “ ***“DEVELOPMENT OF INNOVATIVE METHODS AND MECHANISMS FOR ENERGY PIEZOHARVESTERS“***
Circulation: 3 pcs. (English language)

I. GENERAL CHARACTERISTICS OF THE DISSERTATION

Relevance of the issue:

The growing need for energy resources leads to an increased demand for alternative technologies and renewable resources in the field of energy production.

The specifics of industrial energy production determine the great need for fossil fuels, which are being depleted at an increasing rate, and their intensive use also leads to a deterioration of the environmental situation, especially in the locations of energy generating enterprises. Also, with the increased use of compact, mobile devices with advanced functionality, the use of multiple miniature power sources is imposed, which require relatively rare resources and often pose a danger to the environment after their life cycle.

Mechanical energy is widely distributed in the environment and can be converted into useful electrical energy. Piezoelectric conversion is the most significant mechanism for collecting mechanical energy due to its high electromechanical bonding coefficient and piezoelectric coefficient compared to electrostatic, electromagnetic, and triboelectric conversion.environment.

Therefore, this dissertation examines the possibility of creating a miniature generator of electrical energy to be generated by mechanical vibrations that are insignificant or parasitic for a given phenomenon.

Purpose and Task of the Dissertation work

In this regard, the present dissertation aims at creating and optimizing existing models, as well as mathematical modeling of piezoelectric harvesters of vibration and compression type.

The tasks to be solved in this development are:

1. Presentation of a methodology for describing a vibration harvester.
2. Development of monomorphic and bimorphic piezoelectric harvester models.
3. Creation of a methodology for describing a compression piezoelectric harvester.
4. Development of a model of a compression piezoelectric harvester.
5. Experimental studies of the proposed models of piezoelectric harvesters of vibration and compression type.

Research methods

The research methods have the following sequence - analysis of the state of the problem, analysis of existing models of vibration and compression harvesters, optimization and development of new mathematical models, experimental research in order to verify the proposed models.

Scientific novelty

Mathematical models of piezoelectric harvesters of vibration and compression type have been created. The equivalent circuits have been extended in order to determine the usable amount of energy of a vibrating piezoelectric harvester. Two variants of planar construction of a compression piezoelectric harvester and a methodology for their study are proposed.

Applicability

In connection with the development of compression piezoelectric harvesters, a design has been created for more efficient energy harvesting by reducing the distance between the active elements of the harvester, proven by experimental studies.

Approbation of the dissertation work

The proposed models were investigated experimentally, as part of the results obtained in the development of the dissertation were reported at scientific conferences with international participation, three of which were indexed in SCOPUS.

Structure and volume of the dissertation work

The dissertation is structured in an introduction, four chapters, analysis and conclusions, a list of publications provided by the author, as well as a list of the literature cited by the author, as well as a declaration of authorship, and the total volume of the dissertation is 160 pages.

CONTENT OF THE DISSERTATION

CHAPTER ONE - LITERATURE REVIEW OF ENERGY HARVESTERS AND THEIR APPLICATIONS

Table 1.1: Different energy sources for energy harvesters [42]

Energy Source	Energy density	Literature sorces
Acoustic source	0,003 μW/cm^3, за 75Db 0,96 μW/cm^3,	Patel, & Roundy, 2000
Temperature difference	10 μW/cm^3	(Roundy, Steingart, Frechette, 2004)
Radio Frequencies	1 μW/cm^2	(Yeatman, 2004)
Daylight	100 mW/cm^2 (daylight) 100 W/cm^2 (artificial light)	Averaged
Thermoelectric	60 W/cm^2	(Stevens, 1999)
Vibrations (microgenerators)	4 W/cm^3 (human movement – Hz) 800 W/cm^3 (machinery – kHz)	(Mitcheson, Green, Yeatman,& Holmes, 2004)
vibrations (piezoelectric)	200 μW/cm^3	(Roundy, Wright, & Pister, 2002)
Air current	1 μW/cm^2	(Holmes, 2004)
Keystrokes	50 J/N	(Paradiso & Feldmeier, 2001)
Piezocrystals in shoes	330 μW/cm^2	(Shenck & Paradiso, 2001)
Manual electrical. Generators	30 W/kg	(Starner & Paradiso, 2004)

Possible sources of energy for EH are: radio wave background, photovoltaic sources, thermoelectric sources, electrostatic harvesters, electromagnetic harvesters, pyroelectric and piezoelectric harvesters..

3.2 Piezoelectric EN- The piezoelectric effect is when the compression of a piezoelectric material produces electricity. This occurs when there is a conversion of kinetic or mechanical energy due to the deformation of the crystal into electrical energy. Piezoelectric materials can produce electrical energy due to mechanical deformation.

Methods for generating electrical energy from piezoelectric cells

When a piezoelectric element is mechanically loaded, it generates an electrical impulse. There are two ways to generate energy from a piezoelectric element - by pressure or by vibration. The compressive method generates more power than the vibrational method because it involves a direct transfer of energy to the piezoelectric

module, but it is easier to break [68]. Structurally, these devices are implemented in the following way [68, 158]:

It should be noted that all assumptions and representations of piezoelectric structures made so far are aimed at describing and modeling vibration-type harvesters.

The second group of harvesters are of the compression type, in which, in addition to vibration, there is also a direct mechanical deformation of the active medium by the external mechanical force, which leads to additional difficulties and challenges in the process of their modeling.

In Fig. Figure 1.46 presents the design difference between compression and vibration piezoelectric harvesters.

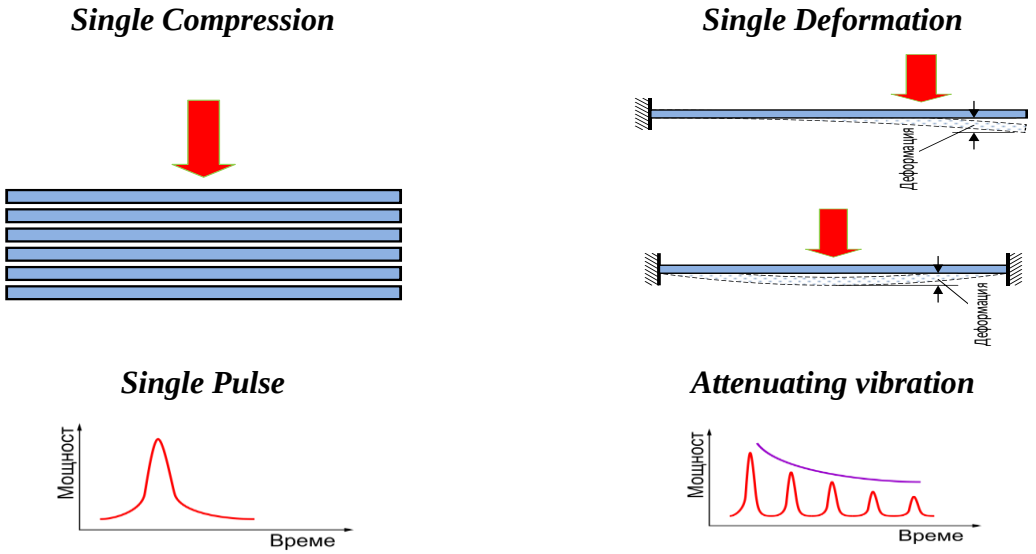

a) compression harvester *b) vibration harvester*

Fig. 1.46 Difference between compression and vibration harvester [158]

There is no proposed universal method for studying the mechanical-electrical connections in PEH. The most commonly used differential equations are to look for relationships between variables in the two domains (mechanical and electrical).

Application of piezoelectric harvester

- • piezoelectric elements built into a shoe
- • piezoelectric elements located on bridge structures
- • Compression piezoelectric harvester model (Fig. 1.50)

Fig. 1.48 Model of a shoe with a piezoelectric console [16]

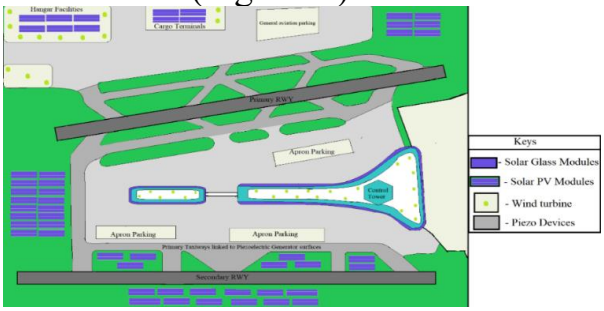

Fig. 1.50 Power generation project prototype [98]

Conclusion

From the literature review, it can be seen that piezoelectric harvesters of vibration and compression type are promising sources for generating electrical energy from our surroundings.

CHAPTER TWO - MATHEMATICAL MODELING OF PIEZOELECTRIC HARVESTERS OF VIBRATION AND COMPRESSION TYPE

2.1.1. Properties of unimorphic and bimorphic PEH

A piezoelectric beam with a rectangular cross-section was chosen.

Table 2.2. Geometric dimensions of a vibrating harvester

a) Single - layer EH PPA-1001	***б) bimorph EH PPA-2014***
*length **(l)** - 55.4 mm*	*length **(l)** - 53.00 mm*
*width **(w)** - 23.4 mm*	*width **(w)** - 23.4 mm*
*thickness **(th)**- 0.46 mm*	*thickness **(th)** - 0.83 mm*
*mass **(m)**- 2.8 g*	*mass **(m)** - 2.9 g*

The following ratios are used: [115]

- To calculate the Young's modulus for the substructural layer- Y_s and the PZT material the dependencies /2.1/ are used Y_p

$$Y_p = \frac{1}{S_{11}^E} = 60.24\ GPa \qquad Y_s = \frac{1}{S_{33}^E} = 47.62\ GPa \qquad /2.1/$$

- The describe the positions relative to the neutral axis h_a, h_b и h_c */2.2/*. It is calculated that for PZT5H *n= 0.79* of the formula /2.1/.

	PPA- 1001	*PPA- 2014*
$h_{pa} = \frac{h_p^2 + 2nh_ph_s + nh_s^2}{2(h_p + nh_s)}$	*0.19*	*0.34*
$h_{sa} = \frac{h_p^2 + 2h_ph_s + nh_s^2}{2(h_p + nh_s)}$	*0.11*	*0.39*
$h_{pc} = \frac{nh_s(h_p+h_s)}{2(h_p + nh_s)}$	*0.12*	*0.16*

/2.2/

Due to the complexity of the mathematical description of systems with variable properties, a restriction will be introduced to consider a beam with the same properties along its length. In this case, the frequency parameter of the harmonics of mechanical oscillation of the beam should be calculated, which will help in describing its deflection, as well as the amplitude of its deflection [36, 38]:

$$1 + \cos i\alpha * \cos\alpha = 0 \qquad /2.4/$$

The subscript (1-4) indicates that the calculation should be done for all four harmonics of the vibrational PEH.

$$\omega_{1-4} = (\alpha_{1-4})^2 \sqrt{\frac{YI}{ml^4}} \qquad /2.6/$$

where ω is the angular frequency, Y is Young's modulus (at constant electrical field of piezoceramics), l is the length of beam, I moment of inertia, m is the ratio of the mass of the piezoharvesters to its length. I and m are found by the formulas:

$$I = \frac{w * th^3}{12} \qquad /2.7/$$

w is the width of the piezoelectric beam and, th is the thickness of the piezoelectric beam.

$$m = \frac{M_p}{l} \qquad /2.8/$$

M_p is the mass of the piezoelectric beam.

After solving equations from /2.4/ to /2.8/ the basic modal parameters of the beam for the individual harmonics (Table 2.4 and Fig. 2.2) of a unimorphic harvester and (Table 2.5 and Fig. 2.3) of a bimorphic harvester are obtained.

Table 2.4. Modal parameters of a single-layer beam

	Frequency Parameter (α)	Modal Constant (σ)	Natural Frequency	
			ω (rad/s)	*f (Hz)*
Harmonic 1	*1,8748*	*0,734*	*13.4977*	*2.1482*
Harmonic 2	*4,6933*	*1,0185*	*84.589*	*13.4628*
Harmonic 3	*7,8534*	*0,999*	*236.8516*	*37.6961*
Harmonic 4	*10,9937*	*1.003*	*464.135*	*73.8693*

Table 2.5. Modal parameters of a bimorph beam

	Frequency Parameter (α)	Modal Constant (σ)	Natural Frequency	
			ω (rad/s)	*f (Hz)*
Harmonic 1	*1,875*	*0,735*	*27,5762*	*4,3889*
Harmonic 2	*4,694*	*1,019*	*172,8169*	*27,5047*
Harmonic 3	*7,854*	*1,001*	*483,8923*	*77,0139*
Harmonic 4	*11,00*	*1.004*	*948,2359*	*150,9164*

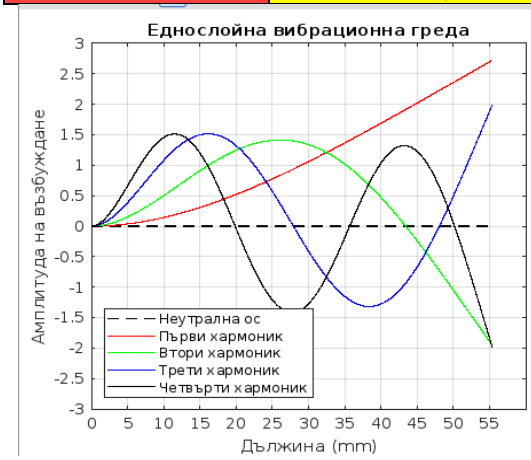

Fig 2.2 Graphical representation of the four harmonics of a single-layer piezoelectric beam

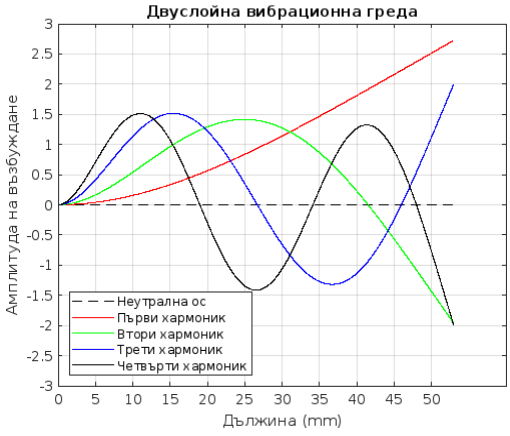

Fig 2.3 Graphical representation of the four harmonics of a two-layer piezoelectric beam

2.2. Modeling a single-layer piezoelectric harvester

2.2.1. Determination of the total deformation of a single-layer beam

To calculate and visualize the deformation of a vibrating beam, the Matlab program was used. To do this, it is necessary to perform the following steps::

1) Entering geometric dimensions of the beam from catalog [161]:

2) Setting the load on beam F in GPa. To show the deformation of the beam at any given time along its entire length, the load is set with an increase step (in this case, 0.5 GPa is selected);

3) Determination of the moment of inertia I beam according to the formula /2.7/

4) Drawing the deformation graph (Fig. 2.4).

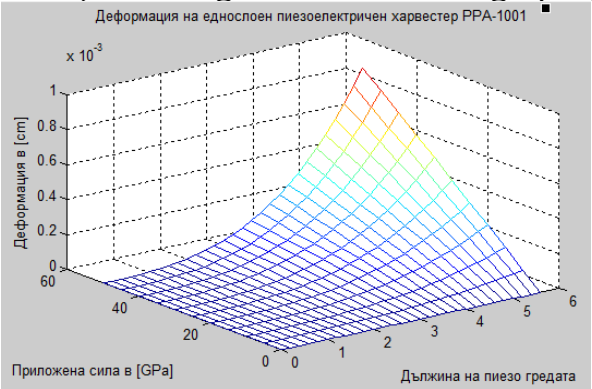

Fig. 2.4. Deformation of PPA-1001

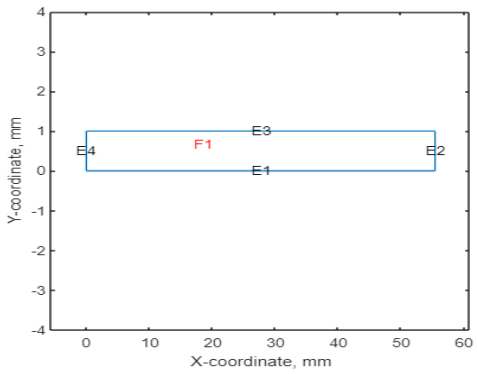

Fig. 2.5. Position of the beam relative to the neutral axis

In Fig. 2.4 shows what the deviation is along the entire length of the vibration beam when an external force is applied to it. It is important to clarify that at its left end the beam is not free, but is attached to the source of vibrations.

2.2.2. Creating a Mathematical Model in a Matlab Environment

In order to analyze the behavior of the piezoelectric part of the harvester, it is required to solve a set of partial differential equations. A single-layer piezoelectric harvester of the company MIDE, model PPA-1001, is being studied, and the piezoceramic material is PZT5H.

To create the mathematical model, the initial conditions [1, 7, 16] are set:

- The direction of polarization points down (negative y-direction) at its top, and points up at its bottom;
- The ratio of the length *l* of the piezo plate to its thickness is *th* is *l/th>100*
- When stress is applied, the beam is deflected in the y direction because its upper part is lengthened and the lower part is shortened. In the z direction, it is the other way around - the upper part is shortened and the lower part is lengthened.
- The left end of the beam is secured, and the right end is free and without inertial load.

The steps by which it is created are:

1) Setting the geometry of the model. For this purpose, the data on the length and thickness of the beam are entered and the method for visualization of the beam itself is set (Fig. 2.5).

2) *Description of material properties.* This is done by introducing Young's modulus (Y), Poisson's coefficient (ν), piezoelectric strain coefficients (d_{31} и d_{33}), the dielectric constant constant of the material, and the dielectric constant in vacuum, the modulus of hardness (G). It is the ratio of Young's modulus to the reaction coefficient of the material (Poisson's ratio).

$$G = \frac{Y}{\nu} \qquad /2.9/$$

3). Input voltage setting..

For the upper part of the beam (voltTop command) edge E3 (Fig. 2.5) a voltage of 100 V is set, and the lower part of the edge E1 (Fig. 2.5) is grounded and there the voltage is zero (voltBot command).

The fact that the left side of the beam is secured is taken into account..

The results obtained are presented in Fig. 2.6, 2.7 and 2.8.

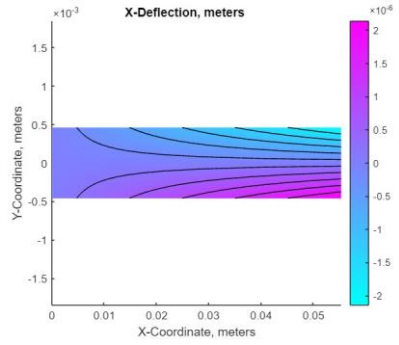

Fig. 2.6 Deformation along the x-axis

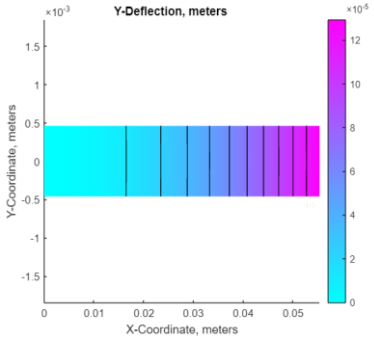

Fig. 2.7 Deformation along the y-axis

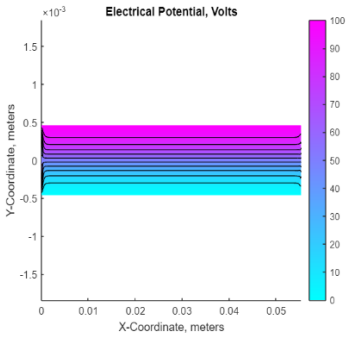

Fig. 2.8 Electric potential of the beam

In Fig. 2.6 shows the deformation of the piezoelectric beam at a voltage of 100V. 2.4 It can be seen that no deformation occurs at the fixed end of the piezo beam when external forces act on it. In Fig. Figure 2.7 shows the deformation of the piezo beam in a transverse form (along the Y-axis). It can be seen that as you approach the free end of the vibrational beam, its deviation increases. In Fig. Figure 2.8 shows the electrical potential of the active layer (pink) and the inactive layer (blue) of the PEH piezoelectric element..

2.2.3. Mathematical modelling of a unimorphic piezoharvester using the finite element method

Piezoceramic PZT5H is a transversely isotropic material.

The basic equations of the piezoelectric medium describe the relationship between mechanical and electrical quantities, usually adopting matrix notations. They can be expressed in two main ways:

- by equations giving the relationship between the tensors of mechanical stresses T_{xyz} and the electric displacement vector D_{xyz} (/2.12/, /2.13/);

through the matrix representation of these equations (/2.14/).

The first way is a description by the components of the voltage tensor T and the vector components of the electric field D and has the form /2.12/ and /2.13/:

$$\{\boldsymbol{T}\} = [\boldsymbol{c^E}]\{\boldsymbol{S}\} - [\boldsymbol{e}]^{\boldsymbol{T}}\{\boldsymbol{E}\} \quad /2.12/$$

$$\{\boldsymbol{D}\} = [\boldsymbol{e}]\{\boldsymbol{S}\} + [\boldsymbol{\varepsilon^S}]\{\boldsymbol{E}\} \quad /2.13/$$

where T is a mechanical stress tensor with 6 components, D is an electrical induction vector with 3 components, S is a mechanical strain vector with 6 components, E is an electrical intensity vector with 3 components, $\boldsymbol{c^E}$ is a mechanical property matrix of size 6×6, $\boldsymbol{\varepsilon^s}$ is an electrical property matrix of size 3×3, and e is a piezoelectric property matrix of size 3×6, and $\boldsymbol{S^E}$ is the coefficient of elasticity [3].

The second way is a matrix description of the type /2.14/:

$$\begin{Bmatrix} T_1 \\ T_2 \\ T_3 \\ T_4 \\ T_5 \\ T_6 \\ D_1 \\ D_2 \\ D_3 \end{Bmatrix} = \begin{bmatrix} c_{11}^E & c_{12}^E & c_{13}^E & 0 & 0 & 0 & 0 & 0 & -e_{31} \\ c_{12}^E & c_{22}^E & c_{23}^E & 0 & 0 & 0 & 0 & 0 & -e_{32} \\ c_{13}^E & c_{23}^E & c_{33}^E & 0 & 0 & 0 & 0 & 0 & -e_{33} \\ 0 & 0 & 0 & c_{44}^E & 0 & 0 & 0 & -e_{24} & 0 \\ 0 & 0 & 0 & 0 & c_{55}^E & 0 & -e_{15} & 0 & 0 \\ 0 & 0 & 0 & 0 & 0 & c_{66}^E & 0 & 0 & 0 \\ 0 & 0 & 0 & 0 & e_{15} & 0 & \varepsilon_{11}^S & 0 & 0 \\ 0 & 0 & 0 & e_{24} & 0 & 0 & 0 & \varepsilon_{22}^S & 0 \\ e_{31} & e_{32} & e_{33} & 0 & 0 & 0 & 0 & 0 & \varepsilon_{33}^S \end{bmatrix} \begin{Bmatrix} S_1 \\ S_2 \\ S_3 \\ S_4 \\ S_5 \\ S_6 \\ E_1 \\ E_2 \\ E_3 \end{Bmatrix} \quad /2.14/$$

For materials whose properties differ along the three orthogonal axes, such as PZT ceramics, the elasticity matrix can be written as follows::

$$S = \begin{pmatrix} \frac{1}{S_{11}^E} & \frac{-v_{13}}{S_{12}^E} & \frac{-v_{12}}{S_{13}^E} & 0 & 0 & 0 \\ \frac{-v_{13}}{S_{21}^E} & \frac{1}{S_{22}^E} & \frac{-v_{31}}{S_{23}^E} & 0 & 0 & 0 \\ \frac{-v_{12}}{S_{31}^E} & \frac{-v_{31}}{S_{32}^E} & \frac{1}{S_{33}^E} & 0 & 0 & 0 \\ 0 & 0 & 0 & \frac{1}{2 * S_{44}^E} & 0 & 0 \\ 0 & 0 & 0 & 0 & \frac{1}{G_6} & 0 \\ 0 & 0 & 0 & 0 & 0 & \frac{1}{2 * S_{55}^E} \end{pmatrix} \quad /2.19/$$

Mode 33 is used for unimorphic piezoelectric harvesters. In this case, the voltage and mechanical load are generated along the z-axis [160].

he Jung modulus of piezoceramics Y_p and of the inactive layer Y_s of PEH can be calculated as follows:

$$Y_p = \frac{1}{S_{11}^E} = 60.24\ GPa \quad /2.20/$$

$$Y_s = \frac{1}{S_{33}^E} = 47.62\ GPa \quad /2.21/$$

Once the values of S_{11}^E, E_{33}^T, S_{33}^E, d_{31} and k_p, are known, the elasticity coefficients S_{12}^E can be found:

$$S_{12}^E = -S_{11}^E + \frac{2d_{31}^2}{k_p^2 E_{33}^T} = -5.7737 * 10^{-12}\ \frac{m^2}{N} \quad /2.22/$$

This makes it possible to find v_p (Poisson's ratio of the piezoelectric layer).

$$v_p = -E_p S_{12}^E = -0.3478 \quad /2.23/$$

$$G_p = \frac{E_p}{2(1 + v_p)} = 40.18\ GPa \quad /2.24/$$

In formula /2.24/ G_p is the modulus of section of piezoceramics.

$$S_{55}^E = \frac{1}{C_{55}^D (1 - k_{15}^2)} = 29 * 10^{-12}\ \frac{m^2}{N} \quad /2.25/$$

$$G_{zp} = \frac{1}{S_{55}^E} = 34.46\ GPa \quad /2.26/$$

$$v_{pz} = \frac{E_p}{E_z} v_{zp} = 0.49 \quad /2.27/$$

$$T_1^P = Y_p (S_1^P - d_{31} E_3) = 9.25 * 10^{11} \quad /2.28/$$

The coefficient of hardness (c) is inversely proportional to the coefficient of elasticity. Therefore: $c_e = s_e^{-1}$.

Table 2.8. Data on elasticity constants taken from a catalogue [15]

S_{11}^E=6,2*10^{10} N/m^2	S_{55}^E=1.7*10^{10}N/m^2
S_{22}^E=Y_{11}^E=6,2 *10^{10} N/m^2	ν_{13}/S_{11}^E=ν_{31}/S_{11}^E=-6.4583*10^{-12}
S_{33}^E=4,9*10^{10} N/m^2	ν=0.31- коефициент на Поасон

From Table 2.8, the elements of the elasticity matrix can be calculated.

$$S = \begin{pmatrix} S_{11} & S_{12} & S_{13} & 0 & 0 & 0 \\ S_{21} & S_{22} & S_{23} & 0 & 0 & 0 \\ S_{31} & S_{32} & S_{33} & 0 & 0 & 0 \\ 0 & 0 & 0 & S_{44} & 0 & 0 \\ 0 & 0 & 0 & 0 & S_{55} & 0 \\ 0 & 0 & 0 & 0 & 0 & S_{66} \end{pmatrix} \qquad /2.36/$$

Here 3 is the ***z***-axis, 2 is the ***y***-axis, and 1 is the ***x***-axis.

Since the catalog data of the piezoelectric harvester do not have data on the coefficients of hardness, they will be calculated using the elastic coefficients (Young's modulus), which are given in the catalog [161].

After replacing the respective coefficients, we get /2.37/:

$$S^E = \begin{pmatrix} 1.613 & -0.646 & -0.516 & 0 & 0 & 0 \\ -0.646 & 2.041 & -0.646 & 0 & 0 & 0 \\ -0.516 & -0.646 & 1.613 & 0 & 0 & 0 \\ 0 & 0 & 0 & 2.9411 & 0 & 0 \\ 0 & 0 & 0 & 0 & 0.423 & 0 \\ 0 & 0 & 0 & 0 & 0 & 2.9411 \end{pmatrix} 10^{-11}\ N/m^2 \qquad /2.37/$$

The inverse matrix of the matrix *"**s**"* is defined and written as the hardness matrix ***„c“***.

$$C = \begin{pmatrix} c_{11} & c_{12} & c_{13} & 0 & 0 & 0 \\ c_{21} & c_{22} & c_{23} & 0 & 0 & 0 \\ c_{31} & c_{32} & c_{33} & 0 & 0 & 0 \\ 0 & 0 & 0 & c_{44} & 0 & 0 \\ 0 & 0 & 0 & 0 & c_{55} & 0 \\ 0 & 0 & 0 & 0 & 0 & c_{66} \end{pmatrix} \qquad /2.38/$$

The resulting coefficients for the hardness matrix are presented in Table 2.9:

Table 2.9. Coefficients for the hardness matrix

c_{11}=c_{31}	0,954*10^{11} N/m^2	c_{22}	0,757*10^{11} N/m^2
c_{12}=c_{21}=c_{23}=c_{32}	0,446*10^{11} N/m^2	c_{44}=c_{66}	0,34*10^{11} N/m^2
c_{13}=c_{31}	0,448*10^{11} N/m^2	c_{55}	0,229*10^{11} N/m^2

The matrix 'd' is composed of the displacement coefficients taken from catalogue [15] for operating mode 33 and presented in Table 2.10:

Table 2.10 Data on relocation rates [161]

Пиезоелектричен коефициент	d_{31}	-320 10^{-12}m/V
	d_{33}	650 10^{-12}m/V
	d_{15}	1000 10^{-12}m/V
	d_{31}=d_{32}; d_{15}=d_{24}	

/2.40/

$$d = \begin{pmatrix} 0 & 0 & 0 & 0 & d_{15} & 0 \\ 0 & 0 & 0 & d_{24} & 0 & 0 \\ d_{31} & d_{32} & d_{33} & 0 & 0 & 0 \end{pmatrix}$$

The electric potential matrix (e) is obtained by multiplying the matrix of piezoelectric coefficients by the hardness matrix.

/2.42/

$$e = \begin{pmatrix} 0 & 0 & 0 & 0 & 22.9 & 0 \\ 0 & 0 & 0 & 34 & 0 & 0 \\ -15.87 & -9.51 & 33.4 & 0 & 0 & 0 \end{pmatrix}$$

/2.43/

$$C_p = \frac{E_{33}^S bl}{h_p} = 2{,}7\ \mu F\ For\ Single\ Layer\ Piezoelectric\ Harvester$$

/2.44/

$$R_p = Q_p \frac{h_p}{bl} = 1T\Omega$$

C_p is the capacitance, and R_p is the resistance ofo piezoceramics.

2.3. Modelling of a bimorphic piezoelectric harvester (PEH)

2.3.1. Determination of the total deformation of a bimorphic beam of PEH The model of a bimorphic harvester created by partial differential equations.

The same methodology is followed as for monomorphic PEH.

1) Entering geometric dimensions of the beam from catalog [161]:
2) Setting the load on the beam (F)
3) Determination of the moment of inertia I beam according to the formula /2.7/
4) Drawing the deformation graph (Fig. 2.9

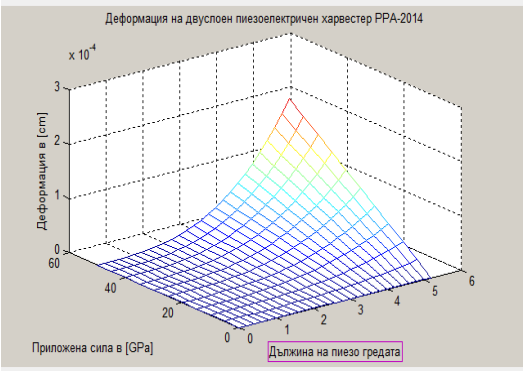

Fig. 2.9 Deformation of a two-layer beam PPA- 2014

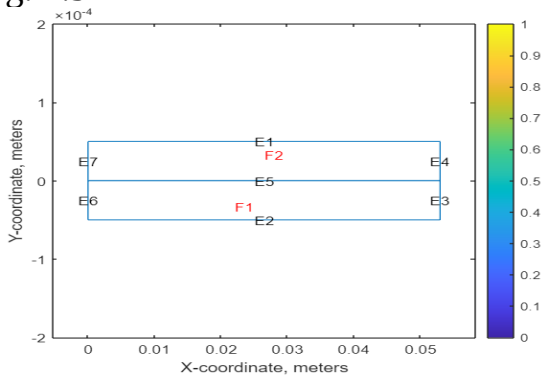

Fig. 2.10. Position of the beam relative to the neutral axis

In Fig. Figure 2.9 shows the deviation along the entire length of the vibration beam when an external force is applied to it.

2.3.2. Creating a Mathematical Model of a Bimorphic Piezoharvester by Using Partial Differential Equations in a Matlab Environment

The mathematical model of a bimorphic piezoelectric harvester by MIDE, type PPA-2014, is created on the basis of a piezoceramic material type PZT5H.

The sequence in creating the bimorphic PEH model is the same as in designing a single-layer PEH beam.

1) The steps by which it is created are:
2) Setting the geometry of the model

3) Description of material properties.
4) Input voltage setting

The results obtained are presented in Fig. 2.11, 2.12 and 2.13.

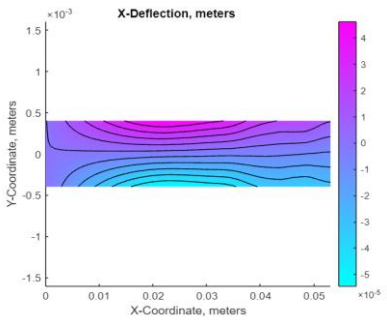

Fig. 2.11 Deformation along the x-axis

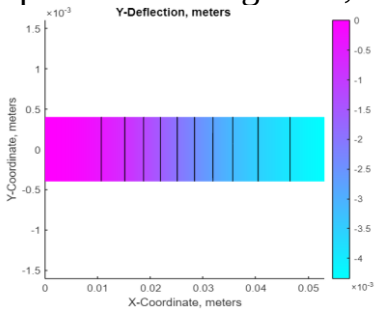

Fig. 2.12 Deformation along the y-axis

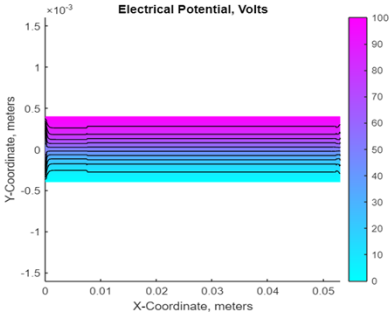

Fig. 2.13 Electric potential of the beam

In Fig. 2.11 shows the deformation of the piezoelectric beam at a voltage of 100V. 2.10 It can be seen that no deformation occurs at the fixed end of the piezo beam when external forces act on it. In Fig. 2.12 is the deformation of the piezo beam in transverse form (along the y-axis). It can be seen that as you approach the free end of the vibrational beam, its deviation increases. In Fig. Figure 2.13 shows the electrical potential of the active layer.

2.3.3. Mathematical modeling of a bimorphic piezoharvester

Bimorphic piezoelectric harvesters operate in the piezoelectric element mode in direction 31. The voltage is generated along the z-axis, and the mechanical load is on the x-axis**.**

$$S_b^E = \begin{pmatrix} \frac{1}{S_{11}^E} & \frac{-v_{12}}{S_{11}^E} & \frac{-v_{13}}{S_{33}^E} & 0 & 0 & 0 \\ \frac{-v_{21}}{S_{21}^E} & \frac{1}{S_{11}^E} & \frac{-v_{33}}{S_{33}^E} & 0 & 0 & 0 \\ \frac{-v_{31}}{S_{33}^E} & \frac{-v_{32}}{S_{33}^E} & \frac{-v_{33}}{S_{33}^E} & 0 & 0 & 0 \\ 0 & 0 & 0 & \frac{1}{2 * S_{44}^E} & 0 & 0 \\ 0 & 0 & 0 & 0 & \frac{1}{2 * S_{55}^E} & 0 \\ 0 & 0 & 0 & 0 & 0 & \frac{1}{G_6} \end{pmatrix} 10^{-11} \frac{N}{m^2} \quad /2.45/$$

With S_b^E the elasticity matrix is marked, the lower index b, indicates that it is a bimorphic beam.

$$S_{11} = S_{22} = \frac{1}{S_{11}^E} = 1{,}613 * 10^{-11}\ N/m^2 \quad /2.49/$$

$$S_{13} = S_{31} = \frac{-v_{13}}{S_{33}^E} = \frac{-v_{31}}{Y_{33}^E} = -0{,}646 * 10^{-11}\ N/m^2 \quad /2.50/$$

$$S_{12} = S_{21} = \frac{-v_{12}}{S_{11}^E} = -0.516 * 10^{-11}\ N/m^2 \quad /2.51/$$

$$S_{33} = S_{23} = \frac{1}{S_{33}^E} = 2{,}041 * 10^{-11}\ N/m^2 \quad /2.52/$$

$$S_{44} = S_{55} = \frac{1}{2S_{44}^E} = \frac{1}{2S_{55}^E} = 2{,}9411 * 10^{-11} N/m^2 \quad /2.53/$$

$$S_{66} = \frac{1}{G_6} = 0{,}423 * 10^{-11}\ N/m^2 \quad /2.54/$$

The number 3 corresponds to the z-axis, the number 2 to the y-axis, and the number 1 to the x-axis.

After substituting the corresponding coefficients in a matrix /2.45/, we get:

$$S_b^E = \begin{pmatrix} 1{,}613 & -0{,}516 & -0{,}646 & 0 & 0 & 0 \\ -0{,}516 & 1{,}613 & 2{,}041 & 0 & 0 & 0 \\ -0{,}646 & 2{,}041 & 0{,}184 & 0 & 0 & 0 \\ 0 & 0 & 0 & 2{,}9411 & 0 & 0 \\ 0 & 0 & 0 & 0 & 2{,}9411 & 0 \\ 0 & 0 & 0 & 0 & 0 & 0{,}423 \end{pmatrix} 10^{-11} \frac{N}{m^2} \qquad /2.55/$$

Therefore, the hardness coefficients can be represented as follows (Table 2.14).

Table 2.14. Coefficients for the hardness matrix

c_{11}	$0{,}691*10^{11}$ N/m^2	$c_{23}=c_{32}$	$0{,}528*10^{11}$ N/m^2
$c_{12}=c_{21}$	$0{,}218*10^{11}$ N/m^2	c_{33}	$-0{,}417*10^{11}$ N/m^2
$c_{13}= c_{31}$	$0{,}0199*10^{11}$ N/m^2	$c_{44}=c_{55}$	$0{,}34*10^{11}$ N/m^2
C_{22}	$0{,}0215*10^{11}$ N/m^2	c_{66}	$2{,}36*10^{11}$ N/m^{2_11}

The matrix 'd' is composed of the displacement coefficients that are taken from a catalogue [161] and presented in Table 2.15.

Table 2.15. Main parameters of piezoceramic PZT5H

Пиезоелектричен коефициент	d_{31}	$-320\ 10^{-12}$m/V	*Диелектрична константа-* K_3^T	3800
	d_{33}	$650\ 10^{-12}$m/V	*Диелектрична проницаемост-* K_3^S	1200
	d_{15}	$1000\ 10^{-12}$m/V	*Механичен фактор на качество-* Q_m	32
	$d_{31}=d_{32}$; $d_{15}=d_{24}$			

In this case $d_{31}=d_{32}$ and $d_{15}=d_{24}$, since PZT ceramics are isotropic in the xy plane.

To calculate *(e)*, the ratio $[e] = [d].[c]$ will be used[196]. As a result, a matrix record of the values of the piezoelectric voltage coefficients (2.58) is obtained..

$$e = \begin{pmatrix} 0 & 0 & 0 & 0 & 34 & 0 \\ 0 & 0 & 0 & 34 & 0 & 0 \\ -16{,}22 & 26{,}6 & -44 & 0 & 0 & 0 \end{pmatrix} \frac{C}{m^2} \qquad /2.58/$$

Table 2.16 Summary of results

$e_{15}=e_{24}=34$ C/m^2	$e_{31}=-16{,}22$ C/m^2
$e_{32}=26{,}6$ C/m^{21}	$e_{33}=-44$ C/m^2

$$C_p = \frac{E_{33}^S bl}{h_p} = 2\ \mu F\ for\ bimorph\ piezoelectric\ harvester \qquad /2.59/$$

$$R_p = Q_p \frac{h_p}{bl} = 1T\Omega \qquad /2.60/$$

2.4 Mathematical modeling of a compression piezoelectric harvester

There are many factors that affect the output power of a harvester, resulting in a lack of a universal way to model them.

In this type of harvesters, it is assumed that the external force acts for short, in most cases repetitive intervals, assuming that the duration of the resulting deformations is commensurate with the times of the external impact. Therefore, the

processes taking place in the piezoelectric structure have an extremely dynamic character, which in a first approximation can be described by sinusoidal or cosine functions.

The factors that affect the energy generated by compression PEH:

- Frequency of movement
- Applied pressure force
- Geometric size of PEH
- Active and passive points of the proposed configuration
- Connection method - series, parallel or combined
- Type of mat that is used to protect the harvester from breakage (hard, soft)
- Depth at which the harvester is located

One of the design options for a compression piezoelectric harvester is the use of a standard piezoelectric resonator [162].

In Fig. 2.14. a standard piezoelectric resonator is presented, with a resonant frequency of 2,9 kHz (±500 Hz), a thickness of 300 μm and a diameter of 25 mm [160, 162] . It is chosen because of its affordability and relatively low cost. The resonator has a metal base with a diameter of 35 mm, which is considered as a simple electrode (black color) [162].

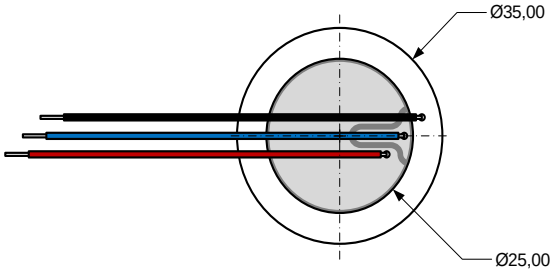

Fig. 2.14. Top view of a compression harvester

Due to the fact that there is no standard approach to determining the average amount of energy received from compression PEH, the methodology [1] for energy reporting [4, 5, 6] is proposed

The methodology includes the following steps::

- *Determination of the force that is applied to a piezoelectric element.*

$$F=m\cdot aN, \qquad /2.61/$$

where *m* is the mass, and *a* is the acceleration. The mass was derived from the average weight of all participants in the experiment.

- *Determination of the charge Q generated in a piezoelectric element.*

$$Q = d_{33} \cdot F[C], \qquad /2.62/$$

where d_{33} is the piezoelectric constant [C/N] and *F* – comprasive force [N].

- *Finding the voltage generated in a piezoelectric element.*

$$U = \frac{Q}{C'}\,[V] \qquad /2.63/$$

where: *C'* – is the capacity of one piezoelectric element.

- *Finding the energy generated by a piezoelectric cell..*

$$W = \frac{C' \cdot U^2}{2} = [J] \qquad /2.64/$$

- *Conversion of the received energy into electrical power P:*

$$P = \frac{W}{t}\ [W] \qquad /2.65/$$

where: t – s the time of impact on the piezoelectric elements in ***s***.

The average impact on piezoelectric elements (the time accepted in experimental studies) is *5 s*.

- *Determination of the electrical power generated by one person's passage through the piezo pad P'.*

Equation /2.66/ contains a constant 2, indicating that electrical power is generated both as a result of pressure (placing the foot) on the piezoelectric element, and as a result of relaxation (displacement of the foot) of the piezoelectric element:

$$P' = 2 \cdot P \cdot n\ [W] \qquad /2.66/$$

where n – is the number of piezoelectric transducers stepped on by the passing person

- *Finding the electrical power generated in a building in a single dayP_D:*

$$P_D = P' \cdot h \cdot m \cdot r\ [W] \qquad /2.67/$$

where: r – is the number of pads located in the respective building, h – is the number of people passing through the pads in one day, m – is the number of passes.

2.5. Conclusions.

2.5.1. A mathematical model has been proposed to help estimate the amount of energy that can be extracted from the proposed energy-generating devices of vibration and compression type.

2.5.2. Vibration piezoelectric harvesters have a classic beam structure with one or two fixed ends and they are the subject of extensive research, both theoretically and experimentally.

2.5.3. Unlike vibrational piezoelectric harvesters, compression harvesters do not have a common design concept. This means a wide variety of constructive solutions, the mathematical models of which can differ radically from each other.

2.5.4. From the mathematical analysis of the piezo track in dynamic mode, it can be seen that the mass of the subject and the time during which pressure is exerted on the piezo element are directly proportional to the output power.

2.5.5. All mathematical models are made for ideal conditions in which mechanical effort is continuous over time, and these mathematical models can THEORETICALLY give the maximum power output for a given structure.

CHAPTER THREE - APPLIED MODELS AND SIMULATION OF PIEZOELECTRIC ENERGY VIBRATION AND COMPRESSION HARVESTERS

3.1 Modeling a vibrating piezoelectric harvester

3.1.1. Modelling of a monomorphic (single-layer) piezoelectric harvester

The static displacement of the piezoelectric console is deduced using the general theory of the Bresse-Kirchhoff-Timoshenko beam, which is based on the assumptions of straightness and non-extensibility. The theory takes into account

shear deformation and rotational bending effects, making it suitable for the description of piezoelectric beams. All conclusions are based on the balance of force and torque of the beam [142].

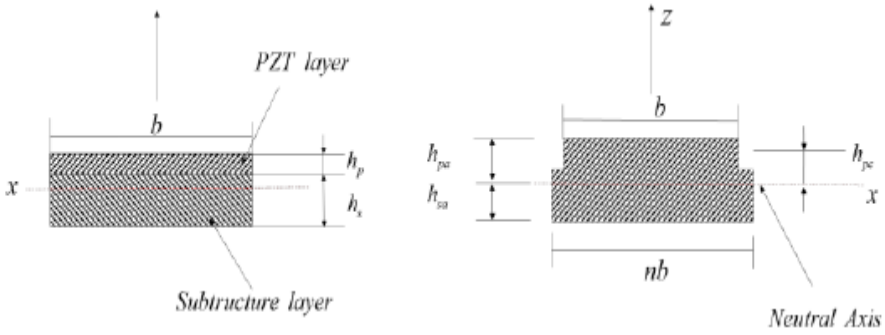

a) structure of single-layer PEH *b) cross-section of single-layer PEH*

Fig. 3.2 Structure and cross-section of single-layer PEH

3.1.2. Related mechanical equation with distributed parameters of a single-layer EH

The initial parameters for the neutral axis should be entered using equations /3.1/, where h_{pa} is the distance from the origin of the PZT layer to the neutral axis, h_{sa} is the distance from the end of the substrate to the neutral axis, and h_{pc} is the distance from the middle of the piezoelectric layer to the neutral axis [115].

$$h_{pa} = \frac{h_p^2+2nh_ph_s+nh_s^2}{2(h_p+nh_s)}, \qquad h_{sa} = \frac{h_p^2+2h_ph_s+nh_s^2}{2(h_p+nh_s)}, \qquad h_{pc} = \frac{nh_s(h_p+h_s)}{2(h_p+nh_s)}, \qquad /3.1/$$

It is generally assumed that the beam system is excited due to movement at the attachment site [125]:

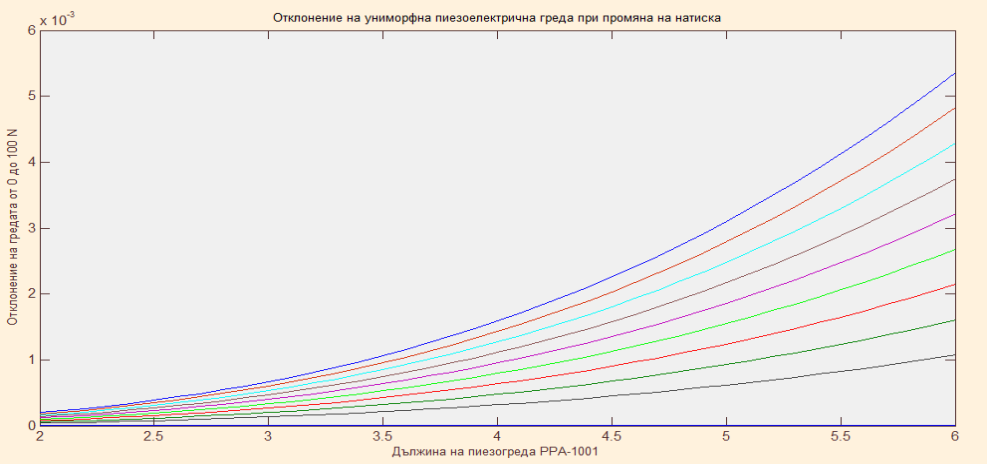

Fig. 3.3 Deviation of a piezoelectric beam to a change in mechanical load

The main equation for motion can then be expressed [125, 136] as:

$$\frac{\partial^2 M(x,t)}{\partial x^2} + c_s I \frac{\partial^5 w_{rel}(x,t)}{\partial x^4 \partial t} + c_a \frac{\partial w_{rel}(x,t)}{\partial t} + m\frac{\partial^2 w_{rel}(x,t)}{\partial t^2} = -m\frac{\partial^2 w_b(x,t)}{\partial t^2} - c_a \frac{\partial w_b(x,t)}{\partial t}, \qquad /3.3/$$

wher $w_{rel}(x, t)$ is the transverse deflection of the beam relative to its base, $M(x, t)$ is the internal bending moment, c_sI is the equivalent damping product for the composite cross-section due to structural viscous elasticity, c_a is the coefficient for fluid-viscous attenuation, and m is mass per unit length of the beam..

The product of bending strength b_{force} f the composite cross-section, provided that a homogeneous electric field is applied to the piezoelectric layer, is:

$$b_{force} = b\frac{Y_s(h_b^3-h_a^3)+Y_p(h_c^3-h_b^3)}{3}. \quad /3.5/$$

The geometric parameters h_a, h_b and h_c describe positions away from the neutral axis (фиг. 3.9,b).

The mass per unit length *m* can be obtained from:

$$m = b(\rho_s h_s + \rho_p h_p), \quad /3.8/$$

where ρ_s and ρ_p are respectively the specific densities of the substructure and the piezoelectric material.

$$\phi_r(x) = \sqrt{\frac{1}{mL}}\left[\cosh\frac{\lambda_r}{L}x - \cos\frac{\lambda_r}{L}x - \sigma_r\left(\sinh\frac{\lambda_r}{L}x - \sin\frac{\lambda_r}{L}x\right)\right], \quad /3.13/$$

where $\phi_r(x)$ and $\eta_r(t)$ respectively are the mass eigenfunction and the modal coordinate function for a beam fixed at one end [19, 38]:

where λ_r is the dimensionless frequency parameter for a given harmonic and is obtained from the following characteristic equation::

$$1 + \cos\lambda\cosh\lambda = 0, \quad /3.14/$$

The modal constant σ_r is expressed as:

$$\sigma_r = \frac{\sinh\lambda_r - \sin\lambda_r}{\cosh\lambda_r - \cos\lambda_r}, \quad 3.15/$$

It should be noted that the above relations /3.13/, /3.14/ and /3.15/ are valid for a beam fixed at one end without additional mass attached to the free end [59, 82].

3.1.3. Equation of an electrical part of a piezoceramic layer under dynamic forces

In order to obtain the equation for the electrical part and its relationship with the mechanical part, it is necessary to consider the basic equations of the piezoelectric medium [36, 76] for the corresponding construction of the piezoelectric EH:

$$D_3 = d_{31}T_1 + \varepsilon_{33}^T E_3, \quad /3.25/$$

where D_3 is the electrical induction, T_1 is the axial force in the piezoelectric layer, E_3 is the electric field component, and ε_{33}^T is the constant force dielectric constant. The axial force T_1 can be expressed as the product of the bending strain S_1 and the Young's modulus of piezoelectricity ($Y_p = \frac{1}{s_{11}^E}$, where s_{11}^E is the elastic correspondence at a constant electric field) using the following fundamental relationship [76]:

$$T_1^p = Y_p(S_1^P - d_{31}E_3). \quad /3.26/$$

After representing the electric field in the piezoelectric layer as a voltage drop on it ($E_3(t) = v(t)/h_p$) and substituting the expressions /3.26/ in the ratio /3.25/, the following equation is obtained:

$$D_3(x,t) = d_{31} Y_p S_1(x,t) - \varepsilon_{33}^S \frac{v(t)}{h_p}. \quad /3.28/$$

The mean bending strain for position ***x*** and time t in the piezoelectric layer can be expressed as a function of the distance hpc from the center of the layer to the neutrality axis and the curvature of the beam for position x and time t with equation /3.29/ [36]:

$$S_1(x,t) = -h_{pc} \frac{\partial^2 w_{rel(x,t)}}{\partial^2 x}. \quad /3.29/$$

Then the expression /3.28/ is amended as follows:

$$D_3(x,t) = -d_{31} Y_p h_{pc} \frac{\partial^2 w_{rel(x,t)}}{\partial^2 x} - \varepsilon_{33}^S \frac{v(t)}{h_p}. \quad /3.30/$$

As is known, the electric current generated in the piezoelectric medium can be expressed as $i(t) = dq(t)/d$, where $q(t)$ is the charge accumulating in the piezoelectric layer. The charge can be obtained by integrating electrical induction over the area of the electrodes [36, 76]:

$$q(t) = \int_0^A D \cdot n dA = -\int_{x=0}^{L} \left(d_{31} Y_p h_{pc} b \frac{\partial^2 w_{rel(x,t)}}{\partial^2 x} + \varepsilon_{33}^S b \frac{v(t)}{h_p} \right) dx, \quad /3.31/$$

where ***D*** is the electric induction vector ***n*** is the external normal and ***A*** is the area of the electrodes.

Since the non-zero products of these vectors are those in the direction of 3 (i.e., in the direction of the y-axis), the current generated in the piezoelectric layer can be expressed as:

$$i(t) = \frac{dq(t)}{dt} = -\int_{x=0}^{L} d_{31} Y_p h_{pc} b \frac{\partial^3 w_{rel(x,t)}}{\partial^2 x \partial t} dx - \frac{\varepsilon_{33}^S b L}{h_p} \frac{dv(t)}{dt}. \quad /3.32/$$

From the expression /3.32/ it is obvious that the generated current is a two-component function, the first component being due to the vibrational movement of the beam (the integral part), and the second reflecting the appearance of a voltage drop in the piezoelectric layer.

$$i(t) = \frac{v(t)}{R_l}. \quad /3.33/$$

On this basis, a simplified equivalent scheme can be created, shown in Fig. 3.9 a). [36]. According to the mathematical model of the vibrational piezoelectric harvester MIDE PPA-1001 developed in Chapter 2, the equivalent circuit shown in Fig. 3.9 (b) is derived.

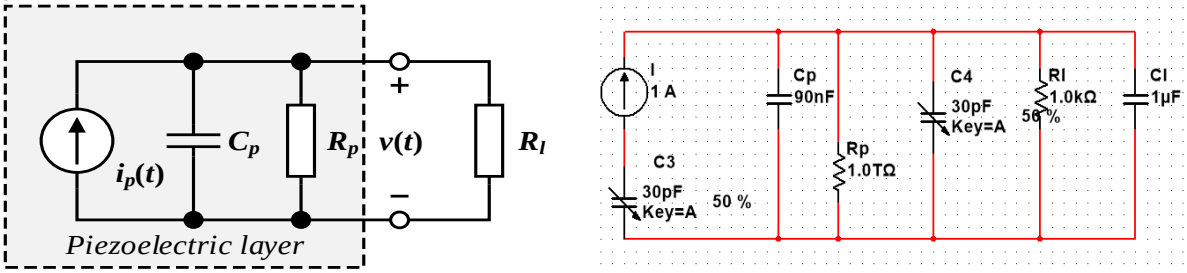

a) a simplified equivalent scheme of single-layer PEH

b) an equivalent scheme of PPA-1001 developed

Fig. 3.4. Equivalent wiring diagram of a single-layer piezoelectric EH

The current source and the alternating capacitance connected to it in series reflect the external mechanical force (C_3). The variable capacitance C3 is selected to reflect the presence of variable external mechanical force. Provided that there is

none, the input of the equivalent circuit will be left open and no energy -R_l (there will be no voltage drop on R_l). Cp is mounting capacities,and both, R_p They represent the parameters of the bimorphic piezo element. C_4 eflects the influences of external capacitances on the operation of the electrical part of the circuit, C_l s put in to accumulate energy. In this way, a higher impedance output is provided to the circuit and internal leaks of the piezo medium are compensated (Fig. 3.4 b)).

$$C_p = \frac{\varepsilon_{33}^S bL}{h_p}, R_p = \varrho_p \frac{h_p}{bL} \quad /3.39/$$

$$i_p(t) = \sum_{r=1}^{\infty} k_r \frac{d\eta_r(t)}{dt}. \quad /3.40/$$

The parameter ϱ_p is the specific resistance of the piezoelectric layer.

3.2. Modeling a bimorphic piezoelectric harvester

3.2.1 Mechanical modeling

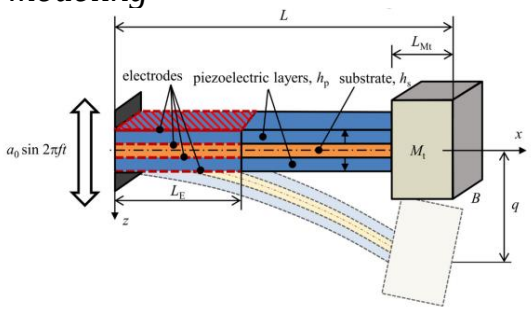

Fig. 3.5. Geometric size of a bimorphic piezoelectric beam in mode 31 [138]

When modeling a bimorphic piezoelectric harvester, analytical solutions for symmetrical bimorphic piezoelectric harvesters with series and parallel connection of piezoceramic layers are considered. It is assumed that the main excitation acting on the bimorphic cantilever piezoelectric element is translation in the transverse direction with a superimposed small rotation.

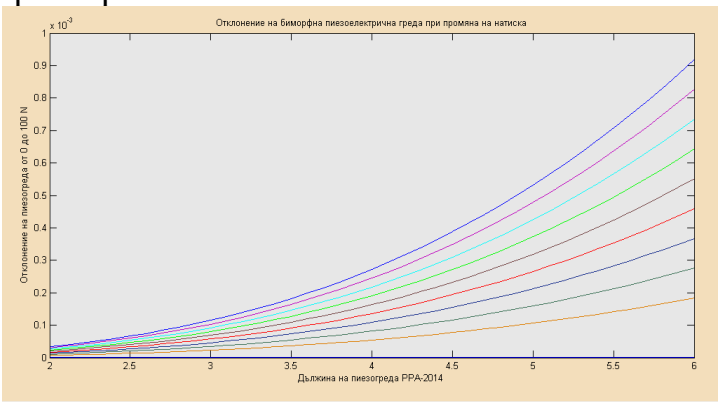

Fig. 3.6. Deviation of a bimorphic piezoelectric beam to a change in mechanical load

It is assumed that the deformations are small and that the composite structure has a linear-elastic behavior of the material (Fig. 3.6). Mechanical losses are represented by internal and external attenuation mechanisms. It is assumed that the internal damping mechanism is in the form of strain damping (Kelvin-Voigt), and the effect of external damping is considered with a separate damping coefficient.

The continuous pairs of electrodes that cover the upper and lower surfaces of the piezoceramic layers are perfectly conductive, which helps to define a single

electrical potential difference through them [22, 30, 39, 96, 107]. Therefore, it is assumed that the input signal for the base motion is constant, so that continuous electrical outputs can be extracted from the electromechanical system..

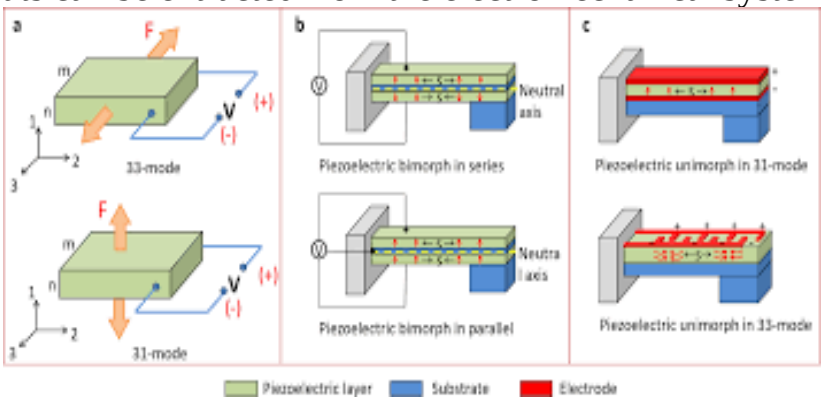

Fig. 3.7. (a) Piezoelectric beam in mode 31 and 33; b) Bimorphic piezoelectric beam with series and parallel connection in mode 31: c) Unimorphic beam in mode 31 and 33 [50]]

From the point of view of mechanics, the bimorphic configurations shown in Fig. 3.7 (b) are identical. This means that they have the same geometric and material properties. However, the effect of the reverse piezoelectric connection in the beam equation is different for the series and parallel connection of the piezoceramic layers, and this has an impact on the piezoelectric beam.

3.2.2. Basic equations of the mechanical par

The movement of the base of each console shown in Fig. 3.7, is represented as translation *g(t)* n the transverse direction with superimposed small rotation *h(t).* Therefore, the effective base displacement *w(x,t)* in the transverse direction can be written as

$$w_b(x,t) = g(t) + xh(t) \qquad /3.41/$$

The partial differential equation describing the forced vibrations of a piezoelectric beam with mass attached to the top and excited by the base can be written as:

$$-\frac{\partial^2 M(x,t)}{\partial x^2} + c_s I \frac{\partial^5 w_{rel}(x,t)}{\partial x^4 \partial t} + c_a \frac{\partial w_{rel}(x,t)}{\partial t} + m\frac{\partial^2 w_{rel}(x,t)}{\partial t^2} = -[m + M_t \delta(x-L)]\frac{\partial^2 w_b(x,t)}{\partial t^2} \qquad /3.42/$$

where $w_{rel}(x,t)$ is the transverse displacement of the beam along the neutral axis relative to its base at position x for time t, c_a is the attenuation coefficient, c_s is the deformation attenuation coefficient, m is the mass per unit length of the beam, M_t is the mass placed at one free end of the piezoelectric beam, $\delta(x)$ is a Dirac function [36].

It is assumed that the bimorphic consoles from Fig. 3.7 are proportionally damped and with normal operation. Therefore, native functions can be used for modal analysis. Instead of specifying the attenuation coefficients in the equation of motion, one can consider the corresponding equation without attenuation (set $c_sI = c_a = 0$ from equation (3.42)) and introduce the modal attenuation into the equation of motion in modal coordinates, as is the practice in structural dynamics [23].

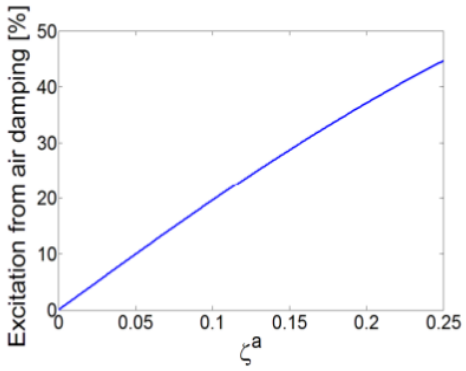

Fig. 3.8 Distribution of excitation from external attenuation to the total excitation term as a function of the coefficient of external attenuation (for excitation at ω = ωn) [36].

The internal bending moment is the first moment of axial deformation in cross-section [36].

$$M(x,t) = b\left(\int_{-h_{\tilde{p}}-\frac{h_{\tilde{s}}}{2}}^{\frac{-h_{\tilde{s}}}{2}} T_1^{\tilde{P}}\, z dz + \int_{\frac{-h_{\tilde{s}}}{2}}^{\frac{h_{\tilde{s}}}{2}} T_1^{\tilde{S}} z dz + \int_{\frac{h_{\tilde{s}}}{2}}^{h_{\tilde{p}}+\frac{h_{\tilde{s}}}{2}} T_1^{\tilde{P}}\, z dz \right) \qquad /3.43/$$

$\boldsymbol{b}$ is the width, $\boldsymbol{h_p}$ is the thickness of each piezoelectric layer. $\boldsymbol{T_1^{\tilde{P}}}$ and $\boldsymbol{T_1^{\tilde{S}}}$ are the components of the axial stress in the piezoceramic layer and in the substrate layer (direction 1=x, longitudinal direction), which is determined by the following dependencies [36]:

$$\boldsymbol{T_1^{\tilde{S}} = Y_{\tilde{s}} S_1^{\tilde{S}}} \quad , \quad \boldsymbol{T_1^{\tilde{P}} = \bar{c}_{11}^{E} S_1^{\tilde{P}} - \bar{e}_{31} E_3} \qquad /3.44/$$

where $\boldsymbol{Y_s}$ is Young's modulus of the substructural layer, $\boldsymbol{\bar{c}_{11}^{E}}$ is the modulus of elasticity of the piezoceramic layer at a constant electric field, $\boldsymbol{\bar{e}_{31}}$ is the effective constant of piezoelectric voltage, and $\boldsymbol{E_3}$ is the component of the electric field in direction 3 ($\boldsymbol{z}$ polarization). Lower and upper subscripts p and s denote the piezoceramic and substructural layer [36].

The axial strain components in the piezoelectric layer as well as in the substructure layer are defined as $\boldsymbol{S_1^{\tilde{P}}}$ and $\boldsymbol{S_1^{\tilde{S}}}$, and are due only to bending [53].

The electric field component $\boldsymbol{E_3}$, must be expressed for both piezoelectric layers of the bimorphic configuration (Fig. 3.8). The two piezoelectric layers are assumed to be the same and the voltage across each layer is $\boldsymbol{u_s(t)/2}$ when connected in series (Fig. 3.7 b, which is located at the top). When the bimorphic piezoelectric harvester operates in mode 31 and is connected in series, $\boldsymbol{\bar{e}_{31}}$ is opposite sign in the two layers due to the opposite polarization, but the instantaneous electric fields are in the same direction $\boldsymbol{E_{3(t)} = \frac{-u_{(t)}}{h_{p1}+h_{p2}}}$. In the parallel connection (Fig. 3.7 b, which is located at the bottom), the voltage on the electrodes of each layer is respectively $\boldsymbol{u_p(t)}$. In this mode, in mode 31 of the bimorphic harvester $\boldsymbol{\bar{e}_{31}}$ as the same sign in both piezoelectric layers, but the instantaneous electric fields are in the opposite direction: $\boldsymbol{E_{3(t)} = \frac{-u_{(t)}}{h_p}}$, for the upper layer and $\boldsymbol{E_{3(t)} = \frac{u_{(t)}}{h_p}}$ for the lower layer.

This is one of the main reasons why the mechanical equations for series and parallel coupling differ from each other. For the internal bending moment of series (M^{ser}) and parallel (M^{par}) coupling, the following equations can be derived [43].

$$M^{ser}(x,t) = b_{force}\frac{\partial^2 w_{rel}^{ser}(x,t)}{\partial x^2} + \vartheta_{ser}u_{ser}(t)\int_{-\infty}^{x}\delta(t)dt \qquad /3.45/$$

$$M^{par}(x,t) = b_{force}\frac{\partial^2 w_{rel}^{par}(x,t)}{\partial x^2} + \vartheta_{par}u_{par}(t)\int_{-\infty}^{x}\delta(t)dt \qquad /3.46/$$

When modeling the piezoelectric harvester in the form of a thin elastic beam, it is important to note that there is no pure bending of the cross-section of the beam. This shows that Bernoulli's hypothesis of the flatness of cross-sections is not valid. When forces act on one end of the beam that deform it, the beam will try to keep its correct shape. This leads to distortions in the cross-sections of the beam, which are closest to the forces causing deformation. As a result of the presence of a shear force in the cross-section of the beam, tangential stresses appear [2].

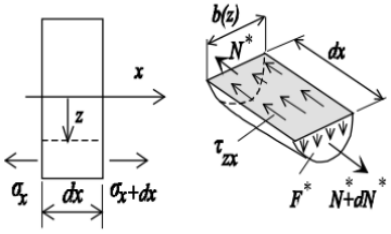

Fig. 3.10. Determination of tangential stresses of the piezoelectric beam [2]

Assuming that the differential element of the beam is of length $\boldsymbol{\Delta x}$, as shown in Fig. 3.10, on the basis of the Zhuravski dependence, it follows that the bending moment - $\boldsymbol{M_y}$ will be a linear or other function of a higher degree, i.e. on both sides of the element the moment will be different, therefore the normal stresses will be different. Due to the inequality of normal voltages, the normal forces acting on the cut off part of the element will not be the same - if on one side the force is N^*, then on the other side is $N^*+\Delta N^*$. In order to be in equilibrium, it follows that tangential stresses act on the longitudinal section of the element- $\boldsymbol{\tau_{zx}}$. This stress is assumed to be uniformly distributed over the width $b(z)$ of the element[2].

$$\sum x = 0 \rightarrow N^* + dN^* - N^* + \tau_{zx}b(z)dx = 0 \rightarrow \tau_{zx} = \frac{dN^*}{b(z)dx} \qquad /3.49/$$

The integral relationship between normal voltage and normal force is:

$$N^* = \int_{F^*}^{th}\sigma_x dF = \int_{F^*}^{th}\frac{M_y}{J_y}zdF = \frac{M_y}{J_y}\int_{F^*}^{th}zdF = \frac{M_y S_y^*}{J_y} \rightarrow \frac{dN^*}{dx} = \frac{d}{dx}\left(\frac{M_y S_y^*}{J_y}\right) = \frac{S_y^*}{J_y}\frac{dM_y}{dx} = \frac{S_y^*}{J_y}Q_z \qquad /3.50/$$

Here S_y^* is the static moment of the cut part of the cross-section with area F^* relative Y-axis of the cross-section of the beam. Substituting in the above equation we get [2]

$$\tau_{zx} = \tau_{xz} = \frac{Q_z S_y^*}{J_y b(z)} \qquad /3.51/$$

The last equation is known as Zhuravsky's formula, which states that the stress will act not only on the planes parallel to the neutral axis, but also in the plane perpendicular to them - the cross-section of the beam.

Using Castigliano's theorem, we can calculate the total potential energy of the beam [3]:

$$U = \int_l \frac{M_y^2}{2EJ_y} ds + k_z \int_l \frac{Q_z^2}{2GF} ds = \frac{1}{2EJ_y} \int_0^l (-P_s)^2 ds + \frac{k_z}{2GF} \int_0^l P^2 ds = \frac{P^2 L^3}{6EJ_y} + k_z \frac{P^2 l}{2GF} \quad /3.52/$$

3.2.3. Connecting equations for the electrical and mechanical parts of the harvester

The basic piezoelectric equations describe the relationship between mechanical and electrical quantities in a piezoelectric medium [195].

$$\{\boldsymbol{T}\} = [\boldsymbol{c^E}]\{\boldsymbol{S}\} - [\boldsymbol{e}]^{\boldsymbol{T}}\{\boldsymbol{E}\} \quad /3.53/$$

$$\{\boldsymbol{D}\} = [\boldsymbol{e}]\{\boldsymbol{S}\} + [\boldsymbol{\varepsilon^S}]\{\boldsymbol{E}\} \quad /3.54/$$

where $\boldsymbol{T}$ is the voltage tensor vector, $\boldsymbol{D}$ is the electrical displacement vector, $\boldsymbol{S}$ is the voltage vector, $\boldsymbol{E}$ is the electrical intensity vector, $\boldsymbol{c^E}$ is the mechanical property matrix, $\boldsymbol{\varepsilon^s}$ is the electrical property matrix, and, $\boldsymbol{e}$ e is the piezoelectric property matrix, and $\boldsymbol{c^E}$ is the elasticity coefficient.

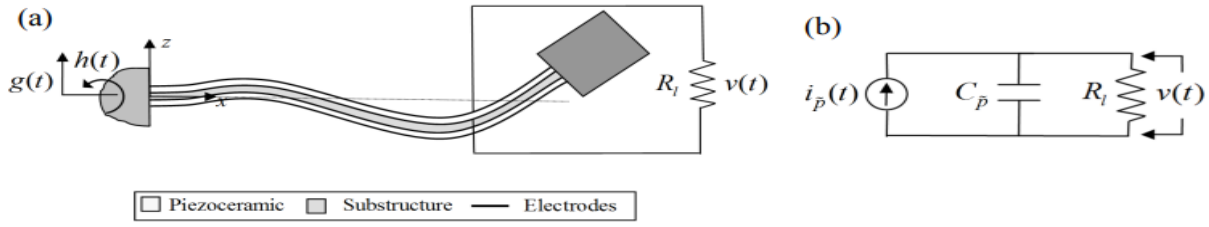

a) connection of the piezoelectric layer *b) equivalent electrical circuit*

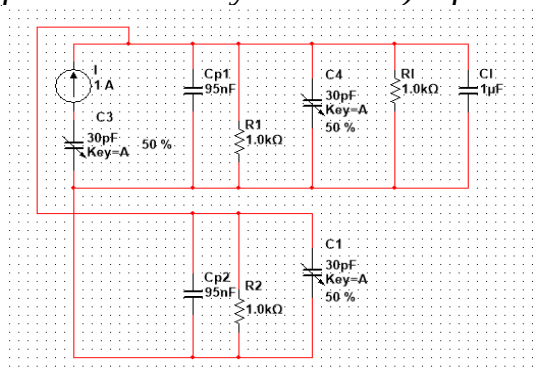

c) developed an equivalent scheme to PPA-2014

Fig. 3.11. Bimorphic structure coupled to a resistive load [36]

The current source and the alternating capacitance connected to it in series reflect the external mechanical force (C_3). The variable capacitance C_3 is selected to reflect the presence of variable external mechanical force. Provided that there is none, the input of the equivalent circuit will be left open and no energy -R_l (there will be no voltage drop on R_l). C_{p1} and C_{p2} are mounting capacities,and both, R_{p1} and R_{p2} are eigenresistances that are connected in parallel. They represent the parameters

of the bimorphic piezo element. C_4 eflects the influences of external capacitances on the operation of the electrical part of the circuit, C_l s put in to accumulate energy. In this way, a higher impedance output is provided to the circuit and internal leaks of the piezo medium are compensated (Fig. 3.11 c)).

The tensor equations (3.53, 3.54 and 3.55) can be expressed in matrix form [86], which is more appropriate when using the finite element method:

$$\begin{Bmatrix} T_1 \\ T_2 \\ T_3 \\ T_4 \\ T_5 \\ T_6 \\ D_1 \\ D_2 \\ D_3 \end{Bmatrix} = \begin{bmatrix} c_{11}^E & c_{12}^E & c_{13}^E & 0 & 0 & 0 & 0 & 0 & -e_{31} \\ c_{12}^E & c_{22}^E & c_{23}^E & 0 & 0 & 0 & 0 & 0 & -e_{32} \\ c_{13}^E & c_{23}^E & c_{33}^E & 0 & 0 & 0 & 0 & 0 & -e_{33} \\ 0 & 0 & 0 & c_{44}^E & 0 & 0 & 0 & -e_{24} & 0 \\ 0 & 0 & 0 & 0 & c_{55}^E & 0 & -e_{15} & 0 & 0 \\ 0 & 0 & 0 & 0 & 0 & c_{66}^E & 0 & 0 & 0 \\ 0 & 0 & 0 & 0 & e_{15} & 0 & \varepsilon_{11}^S & 0 & 0 \\ 0 & 0 & 0 & e_{24} & 0 & 0 & 0 & \varepsilon_{22}^S & 0 \\ e_{31} & e_{32} & e_{33} & 0 & 0 & 0 & 0 & 0 & \varepsilon_{33}^S \end{bmatrix} \begin{Bmatrix} S_1 \\ S_2 \\ S_3 \\ S_4 \\ S_5 \\ S_6 \\ E_1 \\ E_2 \\ E_3 \end{Bmatrix} \quad /3.56/$$

where D_i is the electric displacement vector, E_i is the electric field vector, S_i is the strain vector, and T_i is the voltage vector.

The second alternative way in which the basic equations of the piezoelectric medium of the harvester can be written is:

$$\{\boldsymbol{S}\} = [\boldsymbol{S^E}]\{\boldsymbol{T}\} - [\boldsymbol{d}]^{\boldsymbol{T}}\{\boldsymbol{E}\} \quad /3.58/$$

$$\{\boldsymbol{D}\} = [\boldsymbol{d}]\{\boldsymbol{T}\} + [\boldsymbol{\varepsilon^T}]\{\boldsymbol{E}\} \quad /3.59/$$

Using Riley's beam theory when modeling a thin elastic piezoelectric beam, the only non-zero component of the voltage is the one in the axial direction- T_1.

$$T_2 = T_3 = T_4 = T_5 = T_6 = 0 \quad /3.60/$$

Taking into account that the electrodes cover the area perpendicular to the z-axis and formula 3.60, matrix equation 3.56 can be simplified to:

$$\begin{Bmatrix} S_1 \\ D_3 \end{Bmatrix} = \begin{bmatrix} s_{11}^E & d_{31} \\ d_{31} & \varepsilon_{33}^T \end{bmatrix} \begin{Bmatrix} T_1 \\ E_3 \end{Bmatrix} \quad /3.61/$$

Thus, for the voltage $\boldsymbol{T_1}$ and for the electrical displacement $\boldsymbol{D_3}$ of the piezoelectric beam, it can be written:

$$\begin{Bmatrix} T_1 \\ D_3 \end{Bmatrix} = \begin{bmatrix} \bar{c}_{11}^E & -\bar{e}_{31} \\ \bar{e}_{31} & \bar{\varepsilon}_{33}^S \end{bmatrix} \begin{Bmatrix} S_1 \\ E_3 \end{Bmatrix} \quad /3.63/$$

Since axial deformation is assumed to be the only source of mechanical deformation, the tensor representation of the corresponding piezoelectric dependence can be reduced to a scalar equation [110].

$$D_3 = \bar{e}_{31} S_1^{\tilde{P}} + \bar{\varepsilon}_{33}^S E_3 \quad /3.64/$$

E_3 is the electric field in the direction of polarization (direction $\boldsymbol{z}$).

Here $\bar{e}_{31}$ is the piezoelectric force constant, which is expressed by the piezoelectric strain constant- $\bar{e}_{31} = d_{31}/s_{11}^E$; $\bar{\varepsilon}_{33}^S$ is the dielectric constant at constant deformation, expressed by- $\bar{\varepsilon}_{33}^S = \varepsilon_{33}^T - d_{31}^2/s_{11}^E$; $S_1^{\tilde{P}}$ is a component of axial strain in the piezoelectric layer. Only bending influences it [41].

The mean deformation of the neutral axis ($\boldsymbol{x}$) in the piezoelectric layer is represented as a function of the time $\boldsymbol{t}$ and the distance from the neutral axis to the center of the piezoelectric layer h_{pc}, where $h_{pc} = \frac{h_s + h_p}{2}$.

$$S_1^p(x,t) = -h_{pc}\frac{\partial^2 w_{rel}(x,t)}{\partial x^2} \qquad /3.66/$$

Since the input of the circuit through the electrodes is $\frac{1}{RL}$, the output electric current of the circuit can be obtained from Gauss's law [110].

$$\frac{d}{dt}\left(\int_0^A D_3.ndA\right) = \frac{v(t)}{R_l} \qquad /3.67/$$

where ***A*** is the area of the electrodes and ***D₃*** is the non-zero vector of the electrical displacement in the direction of ***z***. Substituting the expression /3.64/ for the expression /3.67/ the equation with distributed parameters for the electrical circuit is obtained [37].

$$\frac{\bar{\varepsilon}_{33}^S bL}{h_p}\frac{dv(t)}{dt} + \frac{Lb}{\varrho_p h_p}v(t) + \frac{v(t)}{R_l} = -\bar{e}_{31}h_{pc}b\int_{x=0}^{L}\frac{\partial^3 w_{rel}(x,t)}{\partial x^2 \partial t}dx \qquad /3.68/$$

For the transverse vibration reaction, [88, 89]:

$$\frac{\bar{\varepsilon}_{33}^S bL}{h_p}\frac{dv(t)}{dt} + \frac{Lb}{\varrho_p h_p}v(t) + \frac{v(t)}{R_l} = \sum_{r=1}^{\infty} k_r\frac{d\eta_r(t)}{dt} \qquad /3.69/$$

where k_r is the direct correlation coefficient of the direct piezoelectric effect [46].

$$k_r = -\bar{e}_{31}h_{pc}b\int_0^L \frac{d^2\phi_r(x)}{dx^2}dx = -\bar{e}_{31}h_{pc}b\frac{d\phi_r(x)}{dx}\Big|_{x=L} \qquad /3.70/$$

Expression /3.67/ shows that no matter whether a complex circuit or a simple circuit is excited (as in this case), the excitation is proportional to the integral showing the dynamic strain distribution in the electrode region [46, 88, 89]. The application of Kirchhoff's law to the one shown in Fig. 3.16 b chain leads to the expression [36]:

$$C_p\frac{dv(t)}{dt} + \frac{v(t)}{R_p} = i_p(t) \qquad /3.71/$$

C_p is the intrinsic capacity of the piezoelectric layer, and R_p is its own resistance.

The expressions /3.67/, /3.68/ and /3.71/ have an important role in modeling piezoelectric harvesters with beam construction. From them, it can be assumed that at a given number of piezoelectric layers, each of them will have the same capacitance, resistance and current source [36].

3.3. Modeling a compression piezoelectric harvester

It is essential for compression harvesters to design the device so that it has the widest possible resonant band, since the wider the sensitivity spectrum around the resonance value, the more vibrational frequencies are captured in the conversion of mechanical deformation into electrical energy [158].

3.3.1.Mechanical modeling of a compression piezoelectric harvester

In Fig. Figure 3.12 presents the main element of a compression piezoelectric harvester, which is circular in shape.

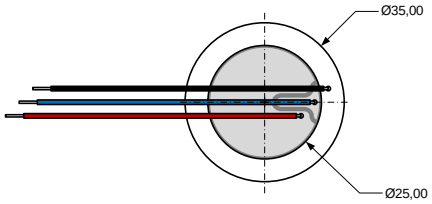

Fig. 3.12. Top view of the piezoelectric element [162]

For the correct modeling of a circular PEH, it is important to find the center of the coordinate system next to the neutral line. For a circular section, the distance from the center of gravity to the tangent to the section will be d/2 [2] Fig. 3.13..

$$\frac{d}{2} = \frac{\frac{4}{\pi d^2}}{\sqrt{\left(\frac{64 y_k}{\pi d^4}\right)^2}} \Rightarrow y_k = \frac{d}{8} \qquad /3.72/$$

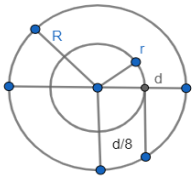

Fig. 3.13. Core of the section of compression PEH

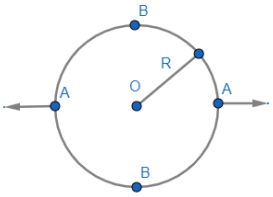

Fig. 3.14. Bending forces in points A and B of compression PEH

The compression harvester is symmetrical and with a symmetrical load. In the vertical plane of symmetry, only bending moment and normal force (x_1) and (x_2) will act. It follows that the efforts at the top and bottom are the same. The force x_2 is found in the equation for statics /3.73/.[2]

$$\sum x = 0 \Rightarrow 2x_2 - P = 0 \Rightarrow x_2 = \frac{P}{2} \qquad /3.73/$$

For the bending moments at points A and B, the following equations apply

$$\mathrm{M} = -\frac{P}{2} R(1 - cos\varphi) \qquad /3.74/$$

$$MA = -\frac{PR}{2} + x_1 \qquad /3.75/$$

$$\mathrm{MB} = x_1 \qquad /3.76/$$

Here ***M*** is the total bending moment, ***MA*** is the bending moment in point ***A***, and ***MB*** is respectively in point ***B***. [3]

The coefficients in the equations /3.74/, /3.75/ and /3.76/ are determined according to the Maxwell-Moore integrals.

$$\delta_{11} = \int \frac{1}{YI_y} R d\varphi = \frac{R\pi}{YI_y} \qquad /3.77/$$

$$\delta_{12} = -2 \int_0^{\frac{\pi}{2}} \frac{PR(1 - cos\varphi)}{2YI_y} R d\varphi = -\frac{PR^2}{YI_y}\left(\frac{\pi}{2} - 1\right) \qquad /3.78/$$

$$\delta_{11}\, x_1 = -\delta_{1p} \qquad /3.79/$$

$$x_1 = \frac{\delta_{1p}}{\delta_{11}} = PR\left(\frac{1}{2} - \frac{1}{\pi}\right) \qquad /3.80/$$

Where ***Y*** is the modulus of elasticity, ***I*** is the moment of inertia, ***R*** is the radius of the disk, and ***δ*** is the linear displacement, where the moment of inertia [3] is found by the formula:

$$I_x = I_y = \frac{\pi d^4}{64} = \frac{\pi r^4}{4} \quad /3.81/$$

3.4.1. Deformation of symmetrical circular PEH

The following dependencies are used in the derivation of compression PEH equations: [58]

- The disc has a constant thickness - th
- The maximum displacement does not exceed th/2, and R≥5th
- The load is axisymmetrical

From Fig. 3.21, the strain equation along the radius of ε_r of compression PEH can be derived..

$$\varepsilon_r = \frac{A'B' - AB}{AB} = \frac{(dr + z(\theta + d\theta) - z\theta) - dr}{dr} = z\frac{d\theta}{dr} \quad /3.82/$$

θ is the angle of rotation of the normal to the middle surface of the plate. The length of the circle passing through point A will undergo a change, which will lead to deformation in the direction of the circle - ε^t. [3]

$$\varepsilon_t = \frac{LA' - LA}{LA} = \frac{2\pi(r + z\theta) - 2\pi r}{2\pi r} = z\frac{\theta}{r} \quad 3.83/$$

The deformation along the radius and in the direction of the circle will give rise to normal stresses σ_r and σ_t, which, according to Hooke's generalized law of plane stress, will be:

$$\sigma_r = \frac{Y}{1-\mu^2}(\varepsilon_r + \mu\varepsilon_t) = \frac{Y_z}{1-\mu^2}\left(\frac{d\theta}{dr} + \mu\frac{\theta}{r}\right) \quad /3.84/$$

$$\sigma_t = \frac{Y}{1-\mu^2}(\varepsilon_t + \mu\varepsilon_r) = \frac{Y_z}{1-\mu^2}\left(\mu\frac{d\theta}{dr} + \frac{\theta}{r}\right) \quad /3.85/$$

From formulas /3.84/ and /3.85/ it can be concluded that the stresses are linearly distributed along the thickness of the plate.

The uneven distribution of stresses on the plane will give rise to bending moments, which we will consider to act on a unit length. These moments will be:

$$M_r r d\varphi = \int_{\frac{-h}{2}}^{\frac{h}{2}} (\sigma_r r d\varphi dz) z \qquad M_t dr = \int_{\frac{-h}{2}}^{\frac{h}{2}} (\sigma_t dr dz) z \quad /3.86/$$

Where after substitution it occurs:

$$M_r = D\left(\frac{d\theta}{dr} + \mu\frac{\theta}{r}\right) \qquad M_t = D\left(\mu\frac{d\theta}{dr} + \frac{\theta}{r}\right) \quad /3.87/$$

Here D is the stiffness of the plate and is located by the formula $D = \frac{Ih^3}{12(1-\mu^2)}$. Using the bending momentsM_r and M_t of the formula /3.87/ for a stress in a specific section of the circle at $z = \pm\frac{h}{2}$ will be obtained:

$$\sigma_{r_{max}} = \pm\frac{6M_r}{h^2} \qquad \sigma_{t_{max}} = \pm\frac{6M_t}{h^2} \quad /3.88/$$

For formula /3.88/ it is important to note that a sign is taken for the lower layer of the compression piezoelectric harvester.

Under shock stress, when an external load with mass (m) is applied for a short time (t), plastic deformation occurs at the place of pressure, which leads to the generation of wave processes, as part of the energy of the external load is dissipated.

At the heart of the energy theory is the assumption that the kinetic energy K_o of pressure is converted into potential deformation energy U without losses to the pressed body, or $K_o = U$. [3]

Shock stress is of two types:

1. Horizontal impact- when a mass of magnitude (m) moves in a straight line with a speed (V) (Fig. 3.17) and hits an elastic body. The mass of the impacting body is significantly greater than the impacted body. The kinetic energy will be $K_o = m_0 \frac{v^2}{2}$, and the potential pressure deformation energy will be:

$$U = \frac{1}{2} P_{max} f_{din} = \frac{1}{2} P_{max} P_{max} \delta_{11} = \frac{1}{2} P_{max}^2 \delta_{11} \qquad /3.89/$$

Where the maximum impact force is $P_{max} = V\sqrt{\frac{m}{\delta_{11}}}$, and maximum dynamic movement is $f_{din} = P_{max}\delta_{11} = V\sqrt{m\delta_{11}}$.

Fig. 3.17. Compression harvester subjected to horizontal impact

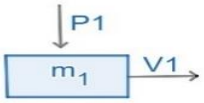

Fig. 3.18. Compression harvester subjected to vertical impact

2. Vertical impact – a mass of size (m_1) and velocity (V_1 falls on an elastic deformable body (Fig. 3.18). The equation of energy balance will be: $K_o + U_{E_{1-2}} = U$, where $U_{E_{1-2}}$ is the change in the potential energy of the impacting body from the moment of impact to the complete deformation of the impacted body and is located from: $U_{E_{1-2}} = mgf_{din}$. Thus, for the potential energy of deformation of the impacted body, the following is obtained: [58]

$$U = \frac{1}{2} P_{max} f_{din} = \frac{1}{2} \frac{f_{din}}{\delta_{11}} f_{din} = \frac{1}{2} \frac{f_{din}^2}{\delta_{11}} \qquad /3.90/$$

3.3.2. Електрическо моделиране на компресионен ПЕХ

As mentioned in Chapter 2, the most efficient way to generate electrical energy is when the compression harvester is subjected to mechanical stress at short, repetitive intervals.

Here the design problem is the efficient distribution of the active elements on the selected area of the piezoelectric harvester, in which with a minimum number of elements to generate the largest possible amount of electrical energy.

The factors that indicate the influence and must be taken into account when constructing a compression piezoelectric harvester are:

- Foot size of passing pedestrians
- **"way" to stepping**
- **the weight** of those passing through the harvester
- **the effort exerted per unit area**
- **pedestrian spreed**
- **biological sex and age of pedestrians**
- **expected number of passers-by**

- A separate factor that also affects the effort is the fact that human beings most often wear shoes, the dimensions of which are determined by the size and structure of the foot.

The way the individual elements are connected is also of key importance, assuming that the series connection will lead to an increase in the amplitude of the received signal (Fig. 3.20 b), and the parallel connection will lead to an increase in the current density obtained from the harvester (Fig. 3.20 a). After preliminary attempts for different ways of connection, it was found that when multiple elements are connected in series, they give a signal when all elements connected in one line are simultaneously compressed, and when even one of them is not compressed, the circuit turns out to be open. Due to the fact that it is not possible to ensure the simultaneous compression of all active elements of the substrate, a parallel type is chosen for the electrical connection, which guarantees the independent operation of all elements of the harvester.

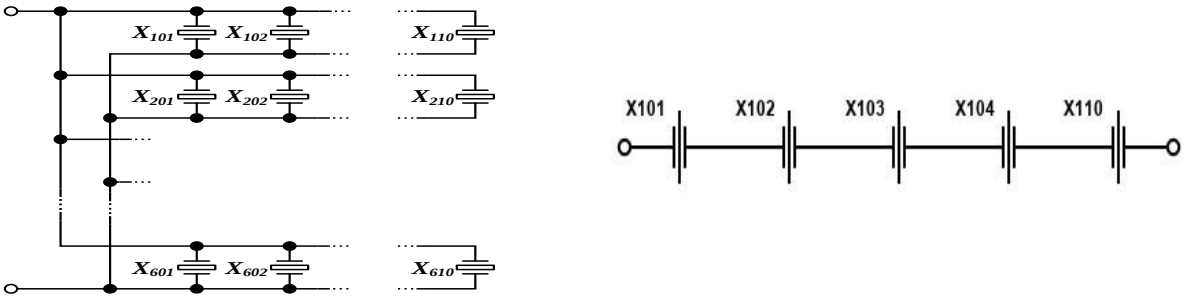

Fig. 3.20. Electrical connection of piezoelectric elements
a) parallel connection *b) serial connection*

The connection used in the harvester is shown in Fig. 3.20 a), and it is obvious that each piezoelectric element can be subjected to mechanical stress, and this will not interfere with the operation of the other elements [1].

3.5. Conclusions

3.5.1. As indicated above in the conclusions of Chapter Two, the models of vibration harvesters are conservative and classical mathematical models for vibration structures are used to describe them. In the present case, these models are supplemented by an extended equivalent scheme, the elements of which describe some of the specific features of beam-type vibration harvesters (Fig. 3.4 b) and Fig. 3.11 (c)).

3.5.2. The accuracy of the classical models for describing vibration harvesters is satisfactory for ideal conditions, but the proposed extended equivalent schemes are intended to reflect the real conditions to which vibrational piezoelectric harvesters may be subjected.

The models of vibration harvesters are extended with an equivalent scheme, while for the proposed design of a compression harvester, a proprietary model is proposed, which is determined by the design features. Based on the model, reasonable assumptions are made that changes in the design of the compression harvester will lead to a change in the generated energy of several orders of magnitude.

CHAPTER FOUR - EXPERIMENTAL STUDIES OF PIEZOELECTRIC HARVESTERS OF VIBRATION AND COMPRESSION TYPE

4.1. Experimental installation for experimental studies of a vibrational piezoelectric harvester (PEH)

Experimental studies have been carried out on the piezoelectric transducer to find out how much power can be extracted from it. For the research, a vibration bench was used, through which mechanical vibrations of different frequencies were provided for influencing the EH.

Experimental studies are carried out with a commercially available piezoelectric harvester [171], which guarantees repeatability of its parameters. The harvester is of the type S233-H5FR-1107XB - a bimorphic structure with serial connection of layers (its previous designation was PPA-2014). To induce the external mechanical impact, an electromechanical vibration stand with an acceleration of a = 5.21 m/s2 is used (Fig. 4.1a), and a functional generator is used to send a harmonic signal through an amplifier to it (Fig. 4.2 b).

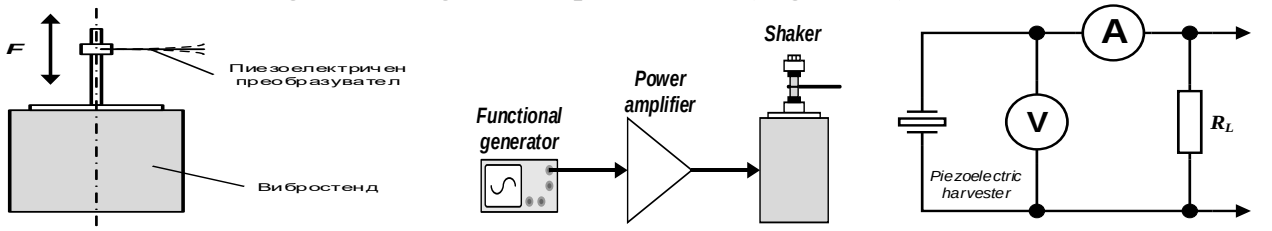

a) Electromechanical vibration test bench *b) Block diagram of the system* *c) Measuring diagram*

Fig. 4.1 Experimental setup

A functional generator is used to change the operating frequency while its output voltage is constant and has a value of 2V pick-to-pick. Measurements are carried out with digital devices that give the corresponding values of the variables in the form of a standard standard value (RMS). This form of data representation is useful because for alternating electric currents and voltages, the effective value is equal to the value of the direct current or voltage, which produces the same average power dissipation over a constant resistive load. Therefore, the power to be measured must be the actual active power that can be easily extracted and is the main purpose of the energy harvesting process.

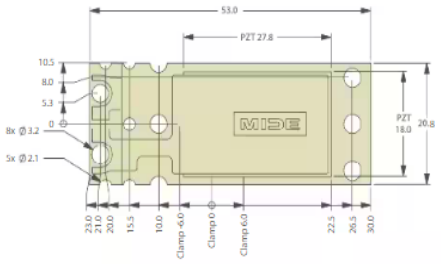

Fig. 4.2 PPA-2014 piezoelectric converter [1]

4.2. Experimental results

The tests were carried out at T=33.8°C, relative humidity - 35%, altitude - 392m.

The first group of experiments was carried out with an inertial mass m=1.13 g with different values of the resistive load (R_L) from 1 to 100 kΩ and a frequency range from 119 to 127 Hz. The initial voltage of the functional generator was 2 V pick-to-pick. The voltage results are in the expected range, but the current values turned out to be strange as they exceeded the expected values (Table 4.4).

Table 4.4 Calculated value of power relative to voltage (P_U), current (P_I) and their product (P_{UI}).

R_l (kΩ)	f, Hz	119	120	121	122	123	124	125	126	127
1	P_U	2,958	2,890	2,856	2,822	2,822	2,993	3,460	3,240	3,028
	P_I	10,824	9,986	9,610	9,425	9,734	11,628	15,210	13,032	11,424
	P_{UI}	5,659	5,372	5,239	5,158	5,242	5,899	7,254	6,498	5,881
2,4	P_U	2,360	2,282	2,301	2,223	2,262	2,731	3,128	2,838	2,625
	P_I	21,744	20,745	20,184	20,045	21,313	28,732	33,034	28,071	25,663
	P_{UI}	7,164	6,880	6,815	6,676	6,943	8,858	10,165	8,926	8,208
5,1	P_U	1,958	1,812	1,836	1,824	1,921	3,013	2,713	2,443	2,240
	P_I	38,850	36,357	36,086	36,357	40,270	68,691	60,001	52,224	46,514
	P_{UI}	8,722	8,117	8,140	8,144	8,795	14,386	12,760	11,296	10,208
7,5	P_U	1,956	1,875	1,976	2,263	3,254	3,034	3,072	2,748	2,442
	P_I	50,311	47,628	52,272	62,641	97,741	87,723	87,723	77,763	68,857
	P_{UI}	9,920	9,450	10,164	11,907	17,833	16,313	16,416	14,619	12,968
10	P_U	1,756	1,747	1,789	1,875	2,352	3,272	2,916	2,601	2,343
	P_I	51,984	52,900	55,225	58,564	77,284	114,244	99,225	87,616	78,400
	P_{UI}	9,553	9,614	9,941	10,479	13,483	19,334	17,010	15,096	13,552
51	P_U	0,928	0,928	0,958	1,042	1,299	1,922	1,711	1,539	1,364
	P_I	72,221	69,814	74,669	82,258	108,712	172,666	150,878	130,560	114,750
	P_{UI}	8,187	8,050	8,458	9,258	11,884	18,216	16,065	14,176	12,510
75	P_U	0,718	0,712	0,754	0,824	1,000	1,549	1,349	1,211	1,082
	P_I	63,480	64,868	64,868	75,000	95,768	164,280	144,908	124,808	106,208
	P_{UI}	6,753	6,798	6,994	7,860	9,786	15,954	13,983	12,294	10,722
100	P_U	0,573	0,566	0,585	0,616	0,848	1,166	1,077	0,933	0,817
	P_I	70,560	73,960	75,690	79,210	121,000	174,240	156,250	139,240	114,490
	P_{UI}	6,359	6,467	6,656	6,987	10,131	14,256	12,975	11,399	9,673

Table 4.5 Graphical representation of power relative to voltage (P_U), current (P_I) and their product (P_{UI}).

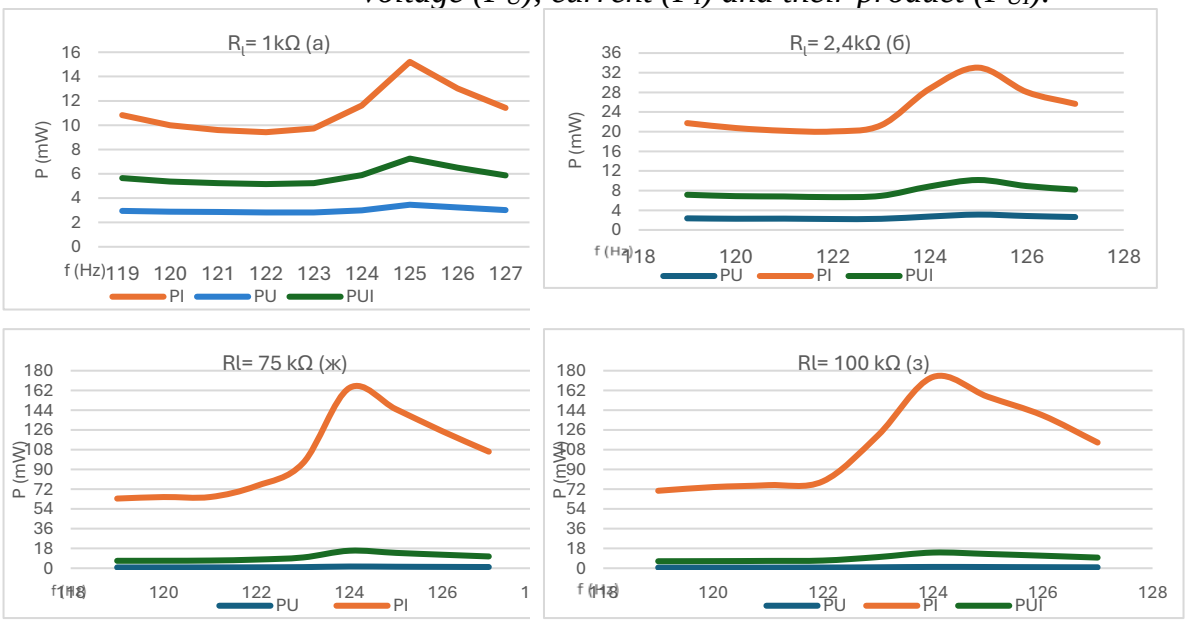

The results for electrical power obtained by indirect methods have such large deviations for both quantities (current and voltage) that the assumption of a defective

experimental setup is necessary. There may be another explanation here: the indicated values are for reactive power, which is available in the system and cannot be used at all [4]. Therefore, for the correct assessment of the energy obtained, it is necessary to straighten the electrical signal of the harvester, and the rectifier must eliminate the influence of reactive energy on the measured results. Therefore, the experimental scheme was expanded with the addition of a rectifier bridge.

4.3 Experimental study of a rectifier bridge circuit

A bridge rectifier and capacitive elements are added to the experimental circuit as shown in Fig. 4.5. The diodes are selected of the 1N4148 type, as they will guarantee a low tripping threshold (low release voltage) and due to the fact that they are high-frequency, their capacitive parameters will not affect the measured results to such an extent. The capacitive elements are selected with a standard value: C_1=1 μF and C_2=1μF, so that they can maintain a voltage at a level that is not affected by rapid changes in the rectifier. The resonant frequency is in the range of 119 - 127 Hz, which is consistent with the inertial load of the harvester. The experimental circuit is divided into DC and AC parts. Experimental circuits can be of the VA and AV types (Fig. 4.5). Due to the fact that there is expected to be a difference in the results obtained from the two measurement schemes, experiments have been carried out to identify the differences and select a more appropriate measurement scheme.

4.3.1 Experimental study of an AV-AV circuit with a rectifier bridge

For the initial measurements with a rectifier bridge, a measurement configuration of type AV-AV was selected (Fig. 4.5).

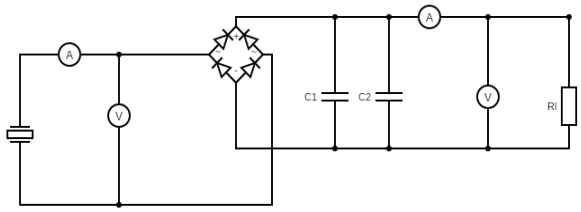

Fig.4.5 Experimental circuit AV-AV with rectifier bridge

4.3.1.1. Experimental study of an AV-AV circuit with a rectifier bridge at C_1=1μF and C_2=1μF

Below are the data on the obtained power results calculated according to the voltage, current and their product (Tables 4.6, 4.7 and 4.8).

Table 4.6 Calculated power versus voltage (P_U) value at C_2=1μF

1 μF	f, Hz	119	120	121	122	123	124	125	126	127
1 kΩ	P_{Udc}	0,281	0,250	0,240	0,240	0,240	0,314	0,423	0,336	0,292
2,4 kΩ	P_{Udc}	0,651	0,651	0,630	0,600	0,641	0,900	1,053	0,900	0,794
5,1 kΩ	P_{Udc}	0,865	0,832	0,816	0,832	0,865	1,559	1,367	1,177	1,037
7,5 kΩ	P_{Udc}	1,145	1,114	1,137	1,479	2,059	2,285	2,101	1,835	1,587
10 kΩ	P_{Udc}	1,204	1,170	1,218	1,332	1,781	1,697	2,247	1,927	1,714
51 kΩ	P_{Udc}	1,142	1,097	1,160	1,283	1,660	2,607	2,266	2,020	1,762
75 kΩ	P_{Udc}	0,950	0,883	0,952	1,082	1,374	2,140	1,972	1,736	1,532
100 kΩ	P_{Udc}	0,814	0,792	0,835	0,918	1,313	1,814	1,615	1,423	1,210

Table 4.9 Calculated power versus voltage (P_U) value at C_2=47 μF.

47 μF	f, Hz	119	120	121	122	123	124	125	126	127
1 kΩ	P_{Udc}	0,624	0,757	0,846	0,846	0,774	0,672	0,640	0,518	0,490
2,4 kΩ	P_{Udc}	1,601	2,054	2,185	2,204	2,054	1,855	1,667	1,504	1,320
5,1 kΩ	P_{Udc}	2,347	3,013	3,216	3,248	2,998	2,743	2,457	2,187	1,933
7,5 kΩ	P_{Udc}	2,883	3,731	4,092	4,181	3,960	3,633	3,267	2,895	2,558
10 kΩ	P_{Udc}	3,226	4,147	4,665	4,706	4,449	4,070	3,660	3,283	2,916
51 kΩ	P_{Udc}	2,805	3,643	4,295	4,518	4,365	4,066	3,696	3,309	2,962
75 kΩ	P_{Udc}	2,292	2,976	3,714	3,763	3,710	3,460	3,142	2,830	2,495
100 kΩ	P_{Udc}	1,831	2,359	2,948	3,031	2,934	2,789	2,481	2,214	1,985

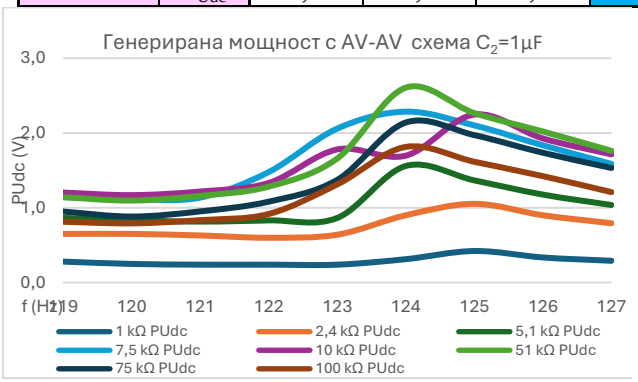

Fig.4.7 Graphical representation of the data from Table 4.6

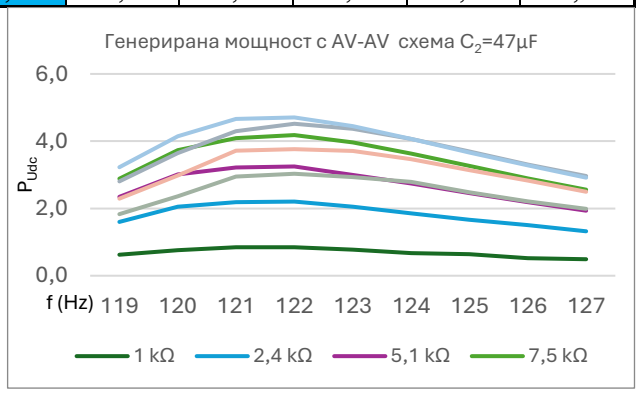

Fig.4.13 Graphical representation of the data from Table 4.9

Table 4.7 Calculated value of power relative to current (P_I) at C_2=1μF.

1 μF	f, Hz	119	120	121	122	123	124	125	126	127
1 kΩ	P_{Idc}	0,297	0,279	0,265	0,257	0,262	0,324	0,434	0,362	0,315
2,4 kΩ	P_{Idc}	0,560	0,544	0,521	0,508	0,539	0,737	0,899	0,761	0,664
5,1 kΩ	P_{Idc}	0,930	0,870	0,853	0,861	0,961	1,722	1,487	1,285	1,122
7,5 kΩ	P_{Idc}	1,135	1,094	1,164	1,432	1,981	2,203	2,020	1,750	1,526
10 kΩ	P_{Idc}	1,116	1,096	1,136	1,239	1,706	2,470	2,107	1,832	1,608
51 kΩ	P_{Idc}	1,014	0,971	1,028	1,132	1,474	2,357	2,040	1,783	1,580
75 kΩ	P_{Idc}	0,780	0,765	0,827	0,908	1,135	1,555	1,621	1,408	1,248
100 kΩ	P_{Idc}	0,884	0,846	0,903	0,960	1,346	1,960	1,742	1,513	1,300

Table 4.10 Calculated value of power relative to current (P_I) at .C_2=47 μF

47 μF	f, Hz	119	120	121	122	123	124	125	126	127
1 kΩ	P_{Idc}	0,787	0,941	1,040	1,040	0,960	0,878	0,799	0,706	0,618
2,4 kΩ	P_{Idc}	1,536	1,918	2,103	2,148	2,036	1,796	1,594	1,434	1,268
5,1 kΩ	P_{Idc}	2,485	3,338	3,642	3,667	3,429	3,119	2,793	2,499	2,208
7,5 kΩ	P_{Idc}	3,024	3,910	4,264	4,355	4,140	3,813	3,437	3,053	2,709
10 kΩ	P_{Idc}	3,295	4,238	4,733	4,747	4,516	4,186	3,733	3,352	2,970
51 kΩ	P_{Idc}	2,721	3,528	4,348	4,468	4,142	3,970	3,581	3,213	2,865
75 kΩ	P_{Idc}	2,271	2,940	3,630	3,730	3,663	3,435	3,030	2,736	2,484
100 kΩ	P_{Idc}	2,220	2,890	3,534	3,725	3,423	3,349	3,028	2,723	2,403

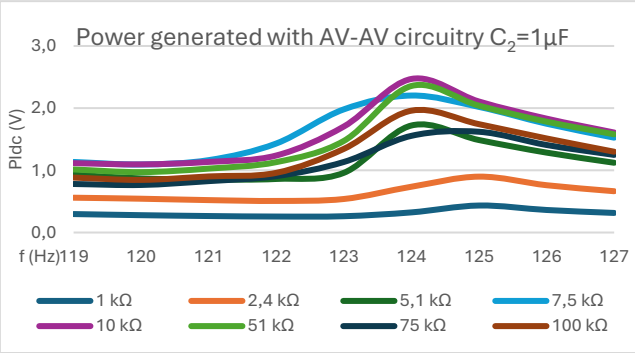

Fig.4.9 Graphical representation of the data from Table 4.7

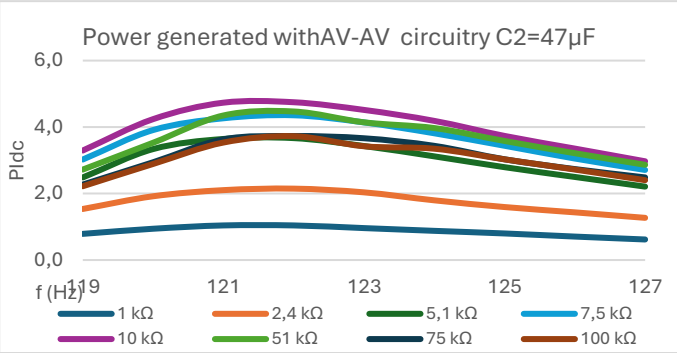

Fig.4.15 Graphical representation of the data from Table 4.10

From the results obtained in the three methods of indirect power generation, it can be seen that the inclusion of a rectifier bridge is justified, since relatively good repeatability of the results for direct current power is obtained.

In order to check the influence of capacitance on the results obtained on DC power, experimental studies were carried out with a change in capacitance after the rectifier bridge. During the experiments, it was found that there was a change in the resonant frequency, which indicates that the capacitance included after the rectifier bridge affects the operating parameters of the harvester.

The studies carried out show that the capacities included in the output circuit have an impact on the amount of energy obtained (Table 4.15 and comparison between Figs. 4.13, 4.15, 4.17 and Figs. 4.19, 4.21, 4.23). This is due to a change in the resonant frequency (Table 4.15), which is within a few Hz, but this is important in energy harvesting systems, which must operate in an optimal mode (when average external mechanical forces lead to the receipt of the maximum amount of electrical energy). Here a complex relationship is observed between the values of the circuit elements and the received energy (Table 4.15).

Table 4.15 Comparison of the resonant frequency at variation of capacitance

	AV-AV wiring diagram								
	1 µF	**47 µF**	**100µF**	**1 µF**	**47 µF**	**100µF**	**1 µF**	**47 µF**	**100µF**
	P_{Udc}			**PIdc**			**PUIdc**		
	f_{res}			**f_{res}**			**f_{res}**		
R (kΩ)	**124**	**122**	**123**	**124**	**122**	**123**	**124**	**122**	**123**
1	0,314	0,824	0,723	0,324	1,04	0,903	0,319	0,938	0,808
2,4	0,9	2,204	2,166	0,737	2,148	2,001	0,814	2,176	2,082
5,1	1,559	3,248	3,377	1,722	3,667	3,599	1,638	3,451	3,486
7,5	2,285	4,181	4,424	2,203	4,355	4,366	2,244	4,267	4,395
10	1,697	4,706	4,665	2,47	4,747	4,638	2,048	4,727	4,651
51	2,607	4,518	2,795	2,357	4,468	2,745	2,479	4,493	2,77
75	2,14	3,763	2,08	1,555	3,73	1,896	1,824	3,746	1,986
100	1,814	3,031	1,713	1,96	3,725	1,96	1,886	3,36	1,833

The first thing that is observed is a change in the resonant frequency, and this change depending on the connection scheme is complex.

The second is the different amount of energy produced by different connection schemes, with the general tendency to produce less energy at smaller external

capacities, connected in parallel to the electrical load. As no complete study of the impact of external capacity has been made, no conclusion can be drawn on the optimal output capacity of the measurement schemes based on the data accumulated so far.

The behavior of the experimental circuits used also shows a complex interconnection, both between the elements of the circuits and the operating modes of the studied vibrational piezoelectric harvester. This should lead to a complication of the model of vibration harvesters of this kind.

4.4. Experimental Setup for Experimental Study of Compression PEH

The experimental studies were carried out at T=21°C, relative humidity - 30% and altitude - 392 m.

Standard piezoelectric resonators with a resonant frequency of 2.9 kHz (±500 Hz), a thickness of 300 μm and a diameter of 25 mm were chosen as primary transducers, due to their affordability and relatively low cost. The piezoelectric elements have a metal base with a diameter of 35 mm, which acts as an electrode.

Piezoelectric harvesters are mounted on a rectangular elastic track made of dielectric material with dimensions of 840 x 540 mm and a thickness of 7 mm.

The two proposed projects are to generate electricity from a piezoelectric walkway, which will be used to collect energy from pedestrians.

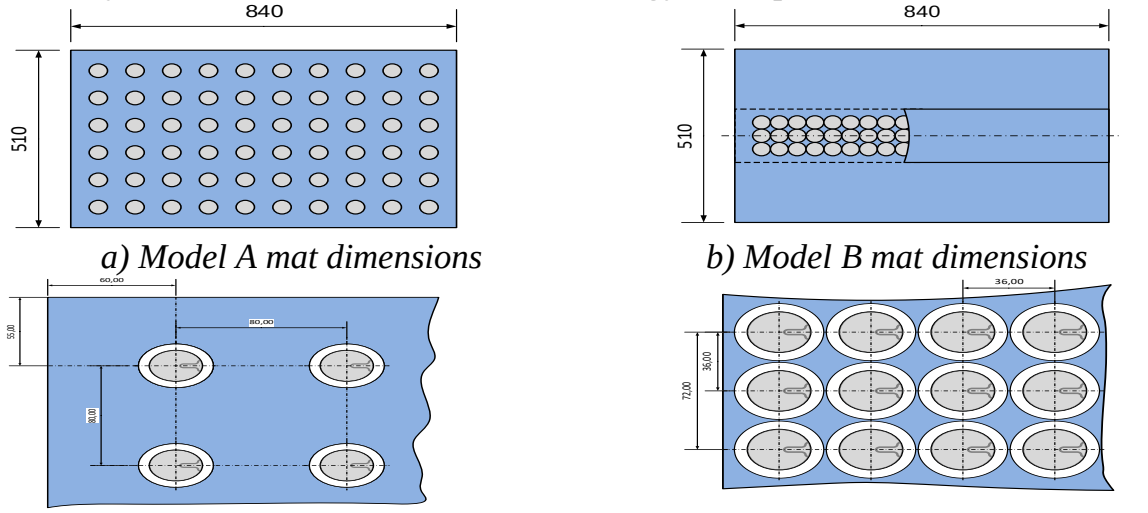

a) Model A mat dimensions *b) Model B mat dimensions*

c) distribution of active elements of Model A *d) distribution of active elements of Model B*

Fig. 4.81. Distribution of active elements

4.5.1. Experimental study with interrupted effects on the piezoelectric path

In design A (Fig. 4.81, c), a quadratic distribution of the elements is selected as shown in, with each element at a distance of 80 mm from the adjacent element. In design B (Fig. 4.81, d), the location of the terminals must be 5 mm apart so that wiring can be carried out without squeezing the wires in order to preserve their integrity. After experiments were carried out on the two options for connecting the elements, it was concluded that only a parallel connection between the elements of the array is applicable, which can guarantee the independent operation of all elements of the harvester.

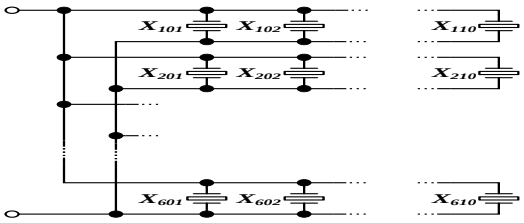

Fig. 4.82. Electrical connection of piezoelectric elements

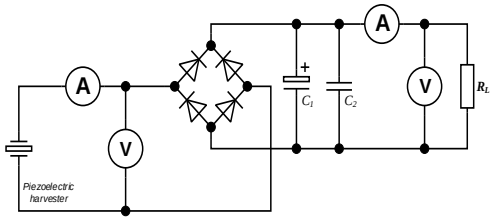

Fig. 4.83. Simplified energy harvesting scheme

To monitor the dynamic component, a DAQ measuring board USB-6001 from National Instruments (NI) is used. The general appearance of the measuring scheme is given in Fig. 4.3, preserving the energy harvesting scheme and monitoring the resulting rectified voltage. In this case, since the input impedance of the analog inputs used on the DAQ board is greater than 1 TΩ, the value of the load resistance is preserved to preserve the ability to calculate the resulting power.

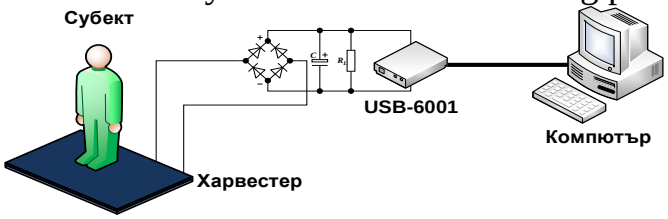

Fig. 4.84. Experimental circuit using a DAQ board

4.5.2 Experimental study of a compression piezoelectric harvester

The measurement is carried out through the program environment of LabView 2023, and the data obtained are in RMS values for the voltage, and the measurement period is set to be 5 s.:

- A group of subjects were interviewed to determine the size of the shoes they wore and were weighed using an electronic scale of the company Silver Crest® type SWG180A1 to determine their weight.
- To conduct the study, subjects shall walk along the length of the substrate within 5 s, taking into account the RMS voltage signal in this time interval (Fig. 4.85).
- Data from the subjects are systematized in tables.

The data for the subject with the corresponding weight and shoe size are given

Table 4.46. Power generated by Model A

измерване	Модел А							
	Маса- 90 кг./ Размер на обувката- 43							
R, kΩ	1	2,4	5,1	7,5	10	51	75	100
1	0,009	0,035411	0,079924	0,716	0,715	1,756	1,951	2,573
2	0,011	0,04328	0,097684	0,654	0,821	1,701	2,039	2,812
3	0,106	0,041706	0,094132	0,594	0,843	1,53	2,184	2,769
4	0,0119	0,079084	0,105677	0,523	0,814	1,642	2,531	3,058
5	0,0201	0,114495	0,178496	0,617	0,901	1,817	2,714	2,811
6	0,0291	0,104265	0,25842	0,653	0,817	1,924	2,439	3,074
7	0,0265	0,076723	0,235331	0,694	0,749	2,017	2,174	3,172
8	0,0195	0,072395	0,173168	0,599	0,804	2,189	2,209	3,249
9	0,0184	0,070428	0,163399	0,638	1,057	1,864	2,473	2,946
10	0,0179	0,0179	0,158959	0,684	0,912	1,799	2,391	3,117
v, RMS	0,02694	0,0655687	0,154519	0,6372	0,8433	1,8239	2,3105	2,9581
P, W	0,0007258	0,0017914	0,0046816	0,0541365	0,0711155	0,0652277	0,0711788	0,0875036

Table 4.47. Power generated by Model B

измерване	Модел Б							
	Маса- 90 кг./ Размер на обувката- 43							
R, kΩ	1	2,4	5,1	7,5	10	51	75	100
1	0,0244241	0,585495	0,644476	0,985	1,173	2,761	3,492	4,695
2	0,051485	0,27243	0,741968	0,892	1,237	2,918	3,278	4,219
3	0,0712786	0,190364	0,828167	1,025	1,204	2,957	3,194	5,091
4	0,0327654	0,399386	0,681056	1,09	1,104	2,801	3,857	5,127
5	0,0655467	0,110025	0,580957	0,993	1,076	2,846	4,215	4,736
6	0,0649433	0,370303	0,65274	1,108	1,281	2,947	3,473	4,679
7	0,117618	0,276929	0,932234	1,031	1,204	2,861	3,284	4,291
8	0,132956	0,354262	0,705948	1,021	1,261	3,024	3,416	4,527
9	0,0998365	0,146905	0,550288	0,843	1,021	2,594	3,578	4,198
10	0,124252	0,382917	0,654218	0,993	1,154	2,654	3,257	4,318
v, RMS	0,0785106	0,3089016	0,6972052	0,9981	1,1715	2,8363	3,5044	4,5881
P, W	0,0061639	0,0397584	0,0953128	0,1328271	0,1372412	0,1577372	0,1637443	0,2105066

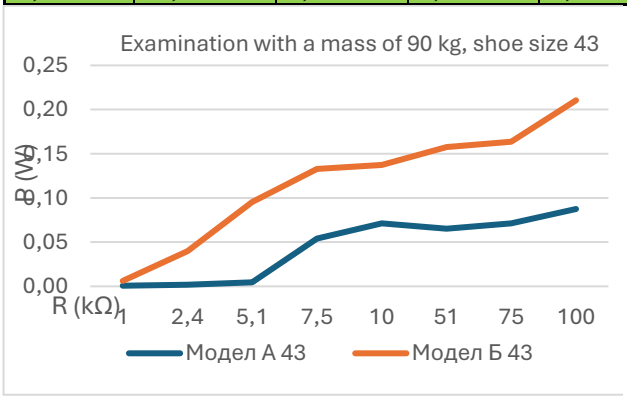

Fig. 4.88. Comparison of Model A and Model B of an entity with a mass of 90 kg. and shoe size - 43

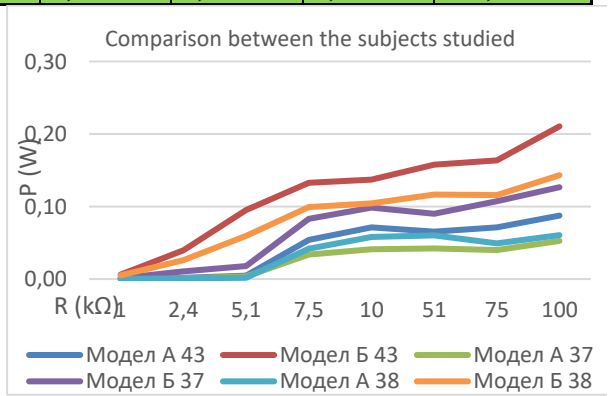

Fig. 4.91. Power generated by Model A and Model B in the study subjects

The data give a very clear idea of how important it is for the correct distribution of active elements on the piezoelectric path, as well as the load resistance in the wiring circuit used. In Model A, the output power in the range from 1 to 5.1 kΩ is negligible, while in Model B, the piezoelectric path generates energy even at a small load resistance. This leads to the conclusion that increasing the mass that will apply pressure to a limited area of the piezoelectric path will lead to an increase in the efficiency of the model (Fig. 4.91).

4.5.3. Continuous Impact Experimental Study on the Piezoelectric Path

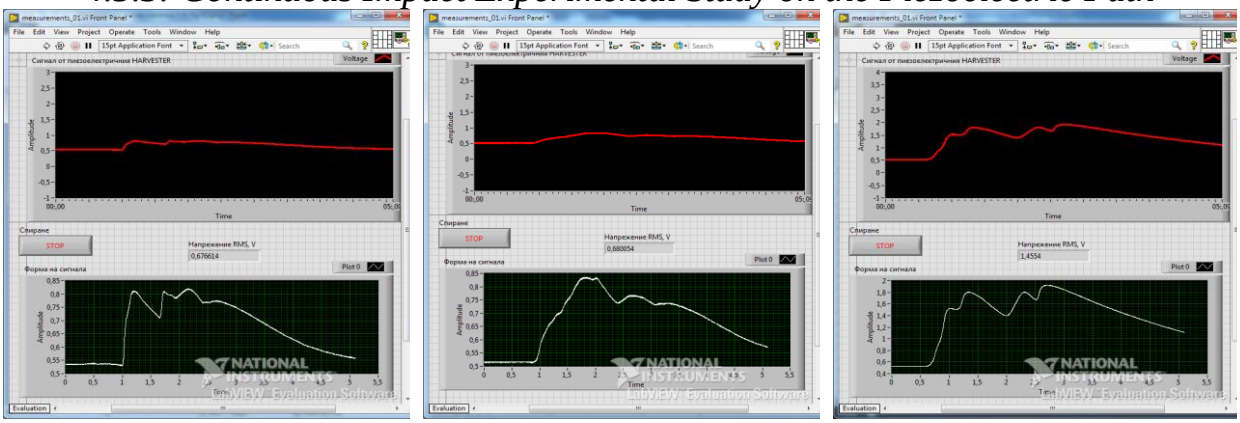

a)an entity with a mass of 60 kg, a shoe size- 37

b)an entity with a mass of 60 kg, a shoe size- 38

c)an entity with a mass of 90 kg, a shoe size- 45

Fig.4.93. Comparison of energy signatures obtained for entities

Based on the methodology from Chapter Two, the generated power from Model A and Model B is presented (Table 4.52). The mass m=83.3 kg was derived from the average weight of the participants in the experiment. The importance of the chosen configuration for the distribution of active elements is clearly visible. With a specified simultaneous pressure on 2.4 times more piezoelectric elements, 2.6 times more output power is generated.

Table 4.52. Generated power output of Model A and Model B

Indicator	Indication	Unit of Measurement	Value	
			Model A	***Model B***
mass	m	kg	83.3	83.3
Impact force	F	N	816	816
Piezoelectric constant, of the piezo element used to build the active pad	d_{33}	C/N	250.10^{-12}	250.10^{-12}
Piezoelectric Cell Capacity	C	F	29.10^{-9}	29.10^{-9}
Time of impact on the piezo pad	t	s	5	5
Number of piezo elements stepped on by one person	n	number	2,5	6
Number of pads in the building	h	number	1	1
Number of passes through the harvester rootstock	m	number	1000	1000
Average number of days per month	D	number	21	21
Power generated by the passage of one person on one piezoelectric element	P'	W	$3{,}5875.10^{-6}$	$3{,}5875.10^{-6}$
Power generated in one day	P_D	W	***0,21***	***0,53***
Power generated in one month	P_M	W	***4,41***	***11,25***
Power generated in one year	P_Y	W	***52,92***	***135***

In the previous study of the compression piezoelectric harvester, pedestrians were used to generate the collected energy. Due to the peculiarities in the movement of human objects, specific features are observed in the profile of the extracted energy (Fig. 4.93). An experiment has been proposed in which this feature is excluded, with the matrix structure being continuously loaded during the study. The location of the applied load on the mold is moved within 5s. Also in the experiment the mass indicators of the device exerting the force were changed.

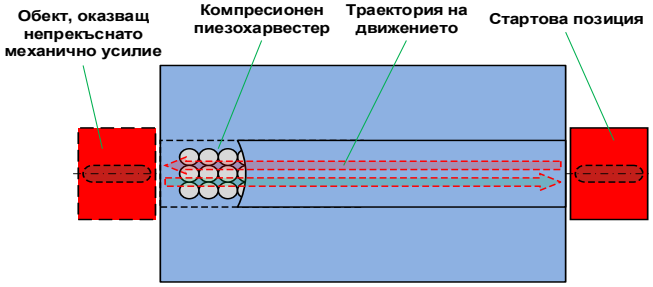

Fig. 4.94. Methodology for conducting the experiment

The measurement methodology is as follows:

- The object through which the mechanical force is applied is initially placed outside the active part of the harvester matrix;
- When starting the experiment within 5s, the moving object is passed along the length of the active part of the matrix (Fig. 4.79. b). The movement is carried out in both directions along this length (Fig. 4.94).

- Each measurement for a certain mass is made 10 times, and the results are averaged. The tables used are four in number, respectively: 15.45 kg., 25.25 kg., 38.25 kg. and 48.05 kg., with the first mass being the mass of the moving object itself.

Table 4.53. Continuous impact power generation with a mass of 15.45 kg.

15,45 kg.										
5sec/kΩ	1	5,1	7,5	10	33,78	51	75	100	240	510
Измерване										
1	0,0113384	0,036239	0,042761	0,095923	0,217146	0,266768	0,156662	0,355397	0,484749	0,707201
2	0,00636512	0,030072	0,047417	0,065527	0,202552	0,419415	0,265473	0,279947	0,27842	0,615941
3	0,00400	0,041048	0,051738	0,058252	0,138231	0,194217	0,355197	0,345013	0,480809	0,722052
4	0,00743571	0,028977	0,078105	0,071928	0,113483	0,193048	0,362787	0,353715	0,613327	0,472364
5	0,00975401	0,03909	0,048743	0,126527	0,124665	0,196443	0,325682	0,337191	0,388514	0,50491
6	0,00574019	0,037648	0,044535	0,089638	0,190753	0,258067	0,231384	0,353593	0,472956	0,549327
7	0,00551553	0,037758	0,057397	0,129233	0,145051	0,160679	0,272563	0,323073	0,421336	0,559918
8	0,00365352	0,037222	0,065358	0,082965	0,1957	0,217036	0,175825	0,389261	0,510563	0,569158
9	0,00673152	0,029191	0,061503	0,078361	0,204744	0,259154	0,251521	0,366366	0,533994	0,487267
10	0,00831428	0,041646	0,041775	0,042896	0,118602	0,301252	0,191139	0,355671	0,565055	0,807462
Средно	0,006884823	0,035889	0,053933	0,084125	0,165093	0,246608	0,258823	0,345923	0,474972	0,59956
P,W	0,000047	0,000253	0,000388	0,000708	0,000807	0,001192	0,000893	0,001197	0,00094	0,000705

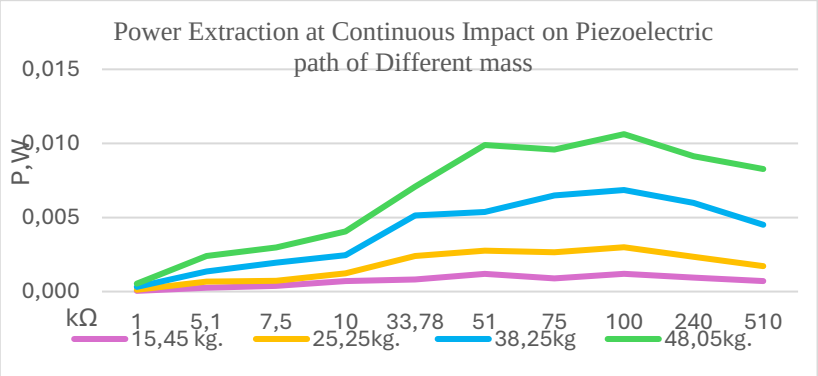

Fig. 4.95 Comparative analysis of power yield at different masses

4.6. Conclusions

4.6.1. A reasonable assumption has been made that part of the energy received is of the reactive type, since by their nature piezoelectric beam vibration harvesters are a resonant structure. In order to confirm this assumption, a rectifier scheme was included in the output circuit of piezoelectric harvesters, through which only the useful direct current power that can be acquired by the harvester was taken into account.

4.6.2. For the specific proposed configuration of a compression piezoelectric harvester, experiments were carried out with interrupted and continuous impact of the active part of the device.

Based on the measurements made, the following conclusions can be drawn:

4.6.2.1. Interrupted impact has been found to be more efficient in obtaining energy from the proposed compression harvester design.

4.6.2.2 Vertical force with interrupted (impact) character achieves better efficiency compared to continuous (horizontal-rotational) impact, which proves the adequacy of the model of compression harvester proposed in Chapter Three (Fig. 3.17 and Fig. 3.18).

4.6.2.3 A larger area of the indicating object leads to the activation of a larger number of active piezoelectric elements, resulting in improved energy efficiency.

ANALYSIS AND CONCLUSIONS

1. A literature review of harvesters using different physical principles of action is made. From the analysis of these harvesters, it can be concluded that those based on the piezoelectric principle give the best ratio between the applied mechanical stress and the resulting voltage drops.

2. Varieties of piezoelectric harvesters are considered, which work on the basis of the forward and reverse piezo effect, but differing in their design features and principle of operation. One of the harvesters under consideration is a classic beam structure using external mechanical vibrations to generate electrical energy, and the second type uses external mechanical deformations to generate electrical energy. Theoretically, the vibration harvester can be considered as a special case of the compression harvester, since the deformation there implies the presence of continuous periodic mechanical effort affecting the structure.

3. The theoretical models of vibrational piezoelectric harvesters are very well developed and are constantly being improved, using them to estimate the maximum possible amount of energy obtained. This is due to the fact that the basic beam structure is conservative and cannot be subjected to such large permutations. All models are based on the Euler-Bernoulli theory of beams, with the more advanced models using the Tymoshenko principle. These models are constantly evolving, and the differences between them most often consist in the electromechanical equivalent circuits used, which take into account the influence of various design features. Most often, the change in these models consists in the connection, the type and number of elements that make up the equivalent circuits, reflecting the electromechanical analogy for piezoelectric media. All mathematical models are created for ideal conditions in which mechanical effort is continuous over time, and these mathematical models can theoretically give the maximum power output for a given structure. These models do not take into account the fact that in real operation of this type of harvester, the mechanical external force may have an interrupted character and the frequency of these efforts may not coincide with the resonance of the first harmonic and may even fall into the field of anti-resonance. This would lead in real conditions to a drastic reduction in the amount of energy extracted.

4. In this work, the equivalent circuit of the classical model of a vibrating piezoelectric harvester is expanded with elements that describe some of the specific features of vibration harvesters of beam type (Fig. 3.9 b) and Fig. 3.16 (c)). The elements of the proposed equivalent schemes reflect some of the variable parameters in the operation of this type of harvesters (such as parasitic capacities), as well as the parameters of the external elements to the scheme, which have an impact on the operation of the harvester. The accuracy of classical models for describing

vibrational harvesters is satisfactorily high for ideal conditions, but the proposed extended equivalent schemes are intended to reflect the real-world conditions to which vibrating piezoelectric harvesters can be subjected.

5. Unlike vibrational piezoelectric harvesters, compression harvesters do not have a common design concept. This means a wide variety of constructive solutions, the mathematical models of which can differ radically from each other. It is customary to create specific mathematical models for the respective constructive solutions, which does not allow the creation of a common mathematical model for this type of harvesters. In this case, a planar construction of a compression harvester is proposed, in which the mechanical force is applied perpendicular to the plane of the arrangement of the elements.

6. For the developed planar construction of a compression harvester, our own model is proposed, based on the basic principles of resistance of materials for vertical and horizontal force. Based on the created model, reasonable assumptions are made that changes in the design of the compression harvester will lead to a change in the generated energy of several orders of magnitude. A change in the harvester structure implies a change in the relative arrangement between the piezoelectric elements, whose parameters remain constant. A connection between the individual elements of the harvester is proposed on a reasonable assumption of the action of the individual piezoelectric elements (Fig. 3.20 a). The series electrical connection of the piezoelectric elements is not appropriate in this case due to the fact that in order to generate a signal for the entire matrix, all elements must be subjected to mechanical pressure at the same time, which is not feasible in the proposed configuration. Therefore, a parallel electrical connection of the piezoelectric elements was used in the construction for further experimental study.

7. To improve the assessment methods, a rectification scheme was included to release only active energy. The experimental results show that this approach is correct, since the results obtained show a great degree of convergence. For comparison, the two classic measurement schemes AV and VA were used, as well as a combination between them to estimate the AC and DC energy received by the harvester device. Only the DC part of the results is used for evaluation.

8. For the proposed planar construction of a compression piezoelectric harvester, studies have been carried out that have a dynamic character. Two types of impacts are used – interrupted and continuous, and the interrupted one refers to the passage of a subject (pedestrian) who passes through the active part with several steps. Continuous impact is understood as the passage of an object performing a horizontal-rotational movement, which is in contact almost continuously with the active part of the harvester.

9. A direct comparison between the proposed designs of a vibration and compression piezoelectric harvester is not applicable due to the fact that the moments of inertia between the two systems are radically different. The inertial mass of the beam vibrational piezoelectric harvester is in the order of several grams, while

the inertial mass of the compression piezoelectric harvester is in the order of tens and hundreds of kilograms.

10. Based on the above conclusion, the different areas of application of the two types of harvesters are defined. The vibration piezoelectric harvester is a system with exceptional inertial sensitivity, which allows it to be used as a sensor at the same time. One of the advantages of compression piezoelectric harvesters is that they have a high degree of scalability, which can be used both to harvest energy from heavy structures and for micro-powers generated by a person in his daily movement, for example, by embedding such a harvester in parts of clothing and shoes. Piezoelectric compression harvester designs can also be used as sensor systems.

CONTRIBUTIONS

Scientific and applied contributions

1. On the basis of the considered physical and mathematical principles of operation of piezoelectric harvesters, it is suggested that piezoelectric vibration beam harvester structures can be considered as a specific special case of piezoelectric compression harvesters.

2. Improved equivalent schemes of a vibrating piezoelectric harvester of beam type have been proposed in order to reflect the real conditions to which this type of structures can be subjected. The elements of the proposed equivalent schemes reflect some of the variable parameters in the operation of this type of harvester (such as parasitic capacities), as well as the parameters of the elements external to the scheme that have an impact on the operation of the harvester.

3. A model of planar construction of a piezoelectric harvester of compression type has been created, which reflects the peculiarities of the elements that make up this device, and is based on the basic principles of resistance of materials for vertical and horizontal force. A parallel electrical connection between the individual elements of the compression harvester is proposed on a reasonable assumption, due to the fact that the series electrical connection of elements in this case is not appropriate, since in order to generate a signal for the entire matrix, all its elements must be subjected to mechanical pressure simultaneously.

4. It is proposed to include a rectifier part in the measurement schemes estimating the amount of energy acquired by harvesters due to obtaining the cost of the obtained experimental results for the obtained AC power. This is due to the presence of a reactive component of power, which leads to an inaccurate reading in indirect methods of estimating the amount of energy received.

5. Two variants of planar construction of a compression piezoelectric harvester and a methodology for their study are proposed. From the studies made, it is proved that the vertical force with interrupted (impact) character achieves better efficiency compared to the continuous (horizontal-rotational) impact, which correlates with the model proposed in Chapter Three..

Applied contributions

6. In connection with the development of compression piezoelectric harvesters, a design has been created for more efficient energy harvesting by

reducing the distance between the active elements of the harvester, proven by the experimental studies.

7. An assessment of the adequacy of the used measurement schemes of the AV and VA type, as well as the combination between them, was made. The results for the DC part show a high degree of convergence, which proves the correctness of the use of a rectifier in the experimental setup.

List of publications related to the dissertation

1. Kolev D., R. Stoyanova, V. Todorova. *„Evaluating the Efficiency of Piezoelectric Energy Harvester of Compression Type*“. Proceedings of X National Conference “ELECTRONICA 2019” May 16-17, 2019, Sofia, IEEE Conference Rec. # 47796, e-ISBN: 978-1-7281-3622-6.

2. Stoyanova R., D. Kolev, V. Todorova. *„Problems in Designing Piezoelectric Compression Harvesters“*. Proc. of ISC UNITECH'2019, 15-16 November 2019, Gabrovo, Vol. 1, pp. 197-201, ISSN 1313-230X.

3. Stoyanova R., “*Estimating Efficiency of Vibrational Piezoelectric Harvester for Human Accessory Integration”* Proc. 13th National Conference with International Participation “Electronica 2022”, May 19-20,2022, Sofia, Bulgaria

4. Stoyanova R., Kolev D., Todorova V., *„Determining the Suitability of Measurement Circuits for Piezoelectric Vibrational Harvesters*“, Proc. XXXI International Scientific Conference Electronics (ET), Sozopol, 2022., ISBN 978-1-6654-9878-4

5. Stoyanova R., D. Kolev, V. Todorova, „Clarification of Utilized Measurement Circuits for Piezoelectric Vibrational Harvesters“, Proc of ISC UNITECH 2022, 18-19 November 2022, Gabrovo, Vol.1 110-115, ISSN 1313-230X